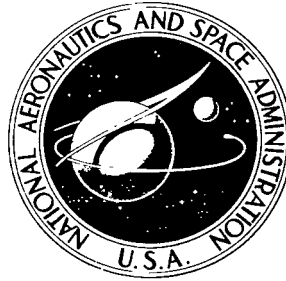


NASA TECHNICAL NOTE



NASA TN D-5753

c. 1

NASA TN D-5753



LOAN COPY: RETURN TO
AFWL (WLOL)
KIRTLAND AFB, N MEX

**POWER-LAW VELOCITY-PROFILE-EXPONENT
VARIATIONS WITH REYNOLDS NUMBER,
WALL COOLING, AND MACH NUMBER
IN A TURBULENT BOUNDARY LAYER**

by Charles B. Johnson and Dennis M. Bushnell

Langley Research Center

Langley Station, Hampton, Va.



0132408

1. Report No. NASA TN D-5753	2. Government Accession No.	3. Recipient's Catalog No.	
4. Title and Subtitle POWER-LAW VELOCITY-PROFILE-EXPONENT VARIATIONS WITH REYNOLDS NUMBER, WALL COOLING, AND MACH NUMBER IN A TURBULENT BOUNDARY LAYER		5. Report Date April 1970	
7. Author(s) Charles B. Johnson and Dennis M. Bushnell		6. Performing Organization Code	
9. Performing Organization Name and Address NASA Langley Research Center Hampton, Va. 23365		8. Performing Organization Report No. L-6757	
12. Sponsoring Agency Name and Address National Aeronautics and Space Administration Washington, D.C. 20546		10. Work Unit No. 129-01-20-07-23	
15. Supplementary Notes		11. Contract or Grant No.	
16. Abstract		13. Type of Report and Period Covered Technical Note	
<p>A survey of turbulent-boundary-layer velocity profiles with zero or slightly favorable pressure gradients was made for Mach numbers up to about 20. The profiles were expressed in terms of the $1/N$-power law for three basic classes of test configurations: (1) flat plates, cones, and hollow cylinders; (2) two-dimensional nozzle walls; and (3) axisymmetric nozzle walls. The values of N were plotted against Reynolds number based on momentum thickness for each of the three classes of configurations and for three groups of wall-to-total temperature ratios ranging from 0.12 to 1.35. It was found that there was generally an "overshoot" in the values of N for data obtained in the region of the beginning of turbulent flow. For profiles downstream of this region, the values of N correlated with Reynolds number based on momentum thickness.</p>		14. Sponsoring Agency Code	
17. Key Words Suggested by Author(s) Turbulent-boundary-layer velocity profile	18. Distribution Statement Unclassified - Unlimited		
19. Security Classif. (of this report) Unclassified	20. Security Classif. (of this page) Unclassified	21. No. of Pages 57	22. Price* \$3.00

*For sale by the Clearinghouse for Federal Scientific and Technical Information
Springfield, Virginia 22151

POWER-LAW VELOCITY-PROFILE-EXPONENT VARIATIONS WITH
REYNOLDS NUMBER, WALL COOLING, AND MACH NUMBER
IN A TURBULENT BOUNDARY LAYER

By Charles B. Johnson and Dennis M. Bushnell
Langley Research Center

SUMMARY

A survey of velocity-profile data from turbulent boundary layers with zero and slightly favorable pressure gradients has been made. Data obtained at Mach numbers up to about 20 have been included in the survey. The profile shapes were characterized according to the $1/N$ -power law and were classified according to three basic types of test configurations: (1) flat plate, cone, and hollow cylinder; (2) two-dimensional nozzle wall; and (3) axisymmetric nozzle wall. The values of N were plotted for each of the three types of configurations with Reynolds numbers based on momentum thickness $R_{e,\theta}$ in three groups of wall-to-total temperature ratio T_w/T_t : (1) $0.66 < T_w/T_t \leq 1.35$; (2) $0.35 < T_w/T_t \leq 0.66$; and (3) $0.12 \leq T_w/T_t \leq 0.35$. A complete tabulation of the data points is included.

The results showed that N is primarily a function of $R_{e,\theta}$ and T_w/T_t . It was also found that when measurements were made in the region of the beginning of turbulent flow ($R_{e,\theta}$ less than approximately 8000), there was generally an "overshoot" in values of N . The available data indicate that the overshoot is most pronounced for flat plates, cones, and hollow cylinders at Mach numbers greater than 4.0 and with near-adiabatic wall-to-total temperature ratios.

For conditions of $R_{e,\theta}$ greater than 8000, the values of N for compressible flows increased with increasing $R_{e,\theta}$ in a manner similar to the results for incompressible turbulent velocity profiles. The wall-temperature effect for all configurations was to increase the values of N for an increase in T_w/T_t .

INTRODUCTION

It has long been recognized from the early experimental work with incompressible turbulent pipe flow by Nikuradse, given in reference 1, that turbulent velocity profiles may be represented by a "power law" of the form $u/u_e = (y/\delta)^{1/N}$. This early pipe-flow work showed that N varied from approximately 6 to 10 as the pipe Reynolds number

was increased. The early pipe-flow work also led to the widespread use of a $1/7$ -power ($N = 7$) law for the representation of flat-plate turbulent boundary layers.

In the integral methods of solving the boundary-layer equations, the $1/N$ -power law has had many applications. Examples of incompressible turbulent-boundary-layer integral solutions using the $1/N$ -power law for the shape of the velocity profiles are given in references 1, 2, and 3. The integral-solution method with $1/N$ -power-law velocity profiles has also been employed extensively for engineering calculations of compressible turbulent boundary layers. Examples of this method, where N is taken as a constant, are given in references 4 and 5. Other integral methods have used empirical correlations of N with Reynolds number based on momentum thickness or a "reference" Reynolds number. (See refs. 6, 7, and 8.) Another method using an N variation is given in reference 9, where N was correlated against the product of the wall-to-total temperature ratio and flow length divided by the momentum thickness for axisymmetric nozzle-wall data. An N correlation with Re_{θ} and T_w/T_t has been used in an integral method in reference 10, where good agreement with experimental profiles was obtained at the test section of several hypersonic axisymmetric nozzles.

In addition to having an application in engineering integral methods, the values of N are useful as an index for the classification and consistency of experimental velocity profiles; that is, the value of N for similar flow conditions on geometrically similar models should be the same. Also, when the velocity profiles are evaluated and cataloged in terms of N , the effect upon profile shape of such basic parameters as wall-to-total temperature ratio, Mach number, and Reynolds number may be assessed.

It is the purpose of this paper to present an evaluation of the variation of N with wall-to-total temperature ratio, Mach number, and Reynolds number, and an effort has been made to include all of the available data known to the authors. The velocity profiles are taken from experiments in which the pressure gradient was either locally zero or slightly favorable. In the process of this evaluation, relationships suitable for use in integral methods (applicable to zero or small pressure-gradient situations only) will be presented. The fairly extensive review and cataloging of the available basic compressible data is useful in that areas can be identified where further data are needed either to establish trends or to prove suspected trends. The experimental data reviewed and used herein are taken from investigations employing the following three classes of configuration: (1) flat plates, cones, and hollow cylinders (hereinafter also referred to as the flat-plate class of flows), (2) two-dimensional nozzle walls, and (3) axisymmetric nozzle walls. The values of N obtained from the data are correlated primarily with Reynolds number based on momentum thickness for three ranges of wall-to-total temperature ratio. Additional correlations at nearly constant values of momentum-thickness Reynolds number show in general the effects of wall temperature on N .

The data available for this survey include the following range of conditions:

- (1) For the flat-plate class of data, $0 \lesssim M_e \leq 16.6$; $1.03 \times 10^3 \leq R_{e,\theta} \leq 1.18 \times 10^5$; and $0.136 \leq T_w/T_t \leq 1.35$
- (2) For the two-dimensional nozzle-wall data, $0.42 \leq M_e \leq 8.18$; $2.25 \times 10^3 \leq R_{e,\theta} \leq 7.02 \times 10^5$; and $0.44 \leq T_w/T_t \leq 1.0$
- (3) For the axisymmetric nozzle-wall data, $0.5 \leq M_e \leq 20.3$; $0.94 \times 10^3 \leq R_{e,\theta} \leq 7.4 \times 10^4$; and $0.12 \leq T_w/T_t \leq 1.0$

SYMBOLS

a	function of $R_{e,\theta}$ (see eq. (2))
b	constant in equation (1)
c	slope of power-law expression (see eq. (2))
M	Mach number
m	slope of linear curve (see eq. (1))
N	velocity-profile power-law parameter
p	pressure
$R_{e,\theta}$	Reynolds number based on momentum thickness, $\frac{u_e \rho_e \theta}{\mu_e}$
$R_{e,x}$	Reynolds number based on x distance, $\frac{u_e \rho_e x}{\mu_e}$
T	temperature
u	velocity component parallel to surface
x	coordinate parallel to the surface
y	distance normal to wall and measured from surface
δ	boundary-layer thickness

θ	momentum thickness
$(\Delta x)_{tr}$	distance parallel to the surface from end of transition to measuring station
μ	viscosity
ρ	density

Subscripts:

e	local external conditions
t	stagnation conditions
w	wall conditions

DETERMINATION OF N VALUES

The value of the N associated with the velocity-profile data was generally found by plotting on log-log paper an actual velocity against a physical distance normal to the wall and obtaining the slope of this curve. The proportionality factors which related the velocity to the distance normal to the wall were taken as the local free-stream velocity u_e and the boundary-layer thickness δ . This thickness is defined herein as the point where a straight-line fairing of the actual velocity on log-log paper intersects the free-stream velocity u_e . Many of the reports that were examined presented the velocity-profile data in some combination of plots, tables, and N -power-law values. In an attempt to obtain consistent values, whenever it was possible, the N value for a particular profile was determined from a new log-log plot of the data taken either from a table or a plot of the data, not from the value given in the report. A straight line was faired through the data over at least the outer 90 percent of the physical boundary-layer thickness δ unless the laminar sublayer extended into this part of the boundary layer. When the sublayer extended into the outer 90 percent of δ , only the outer part of the velocity profile was used to determine the value of N . For investigations where the velocity profiles were not suitably tabulated or plotted for reevaluation, the value of N given in the references was used, as noted in the listing of the data in tables I, II, and III (refs. 9 to 93). It is estimated that the values of N quoted herein have been determined from the data with an accuracy of ± 10 percent.

VARIATION OF N WITH $Re_{e,\theta}$

For the data from flat plates, cones, and hollow cylinders, essentially a zero pressure gradient existed throughout the upstream flow history, whereas for the data from the two-dimensional and axisymmetric nozzle walls, an upstream favorable pressure-gradient history existed with locally either a slightly favorable or zero pressure gradient. However, since the majority of the nozzle data were taken in the nozzle test section, the data generally corresponded to a local zero-pressure-gradient flow. The data for a given class of flow (flat plate, two-dimensional nozzle wall, or axisymmetric nozzle wall) have been shown for each of three ranges of T_w/T_t ($0.66 < T_w/T_t \leq 1.35$; $0.35 < T_w/T_t \leq 0.66$; and $0.12 \leq T_w/T_t \leq 0.35$). Each variation was presented in an attempt to isolate the variation of N with $Re_{e,\theta}$ from possible effects of T_w/T_t . There are not sufficient data available to enable N to be plotted against $Re_{e,\theta}$ at a single value of T_w/T_t .

In the following discussion an "overshoot" in N is said to occur when the N values are appreciably above the usual variation (i.e., greater than customary scatter) of increasing N with increasing $Re_{e,\theta}$ which is exhibited by the incompressible data. It should be noted that correlations of N versus the Reynolds number based on the boundary-layer thickness, the incompressible momentum thickness, and the incompressible displacement thickness were attempted but showed no improvement over the correlation of N versus the momentum-thickness Reynolds number.

Flat-Plate, Cone, and Hollow-Cylinder Data

As indicated previously, the plots showing the variation of N with $Re_{e,\theta}$ are divided into three ranges of wall-to-total temperature ratio: (1) $0.66 < T_w/T_t \leq 1.35$ shown in figure 1; (2) $0.35 < T_w/T_t \leq 0.66$, shown in figure 2; and (3) $0.12 \leq T_w/T_t \leq 0.35$, shown in figure 3. For convenience, the large amount of data for the $0.66 < T_w/T_t \leq 1.0$ range was further subdivided into Mach number ranges of $Me < 4$ (figs. 1(a) and 1(b)) and $Me > 4$ (fig. 1(c)). Figure 1(b) compares the regions of compressible and incompressible data. The key to symbols in these figures is given in table I. Also shown in figures 1 to 3 is the N variation obtained from reference 94.

The data exhibit a great deal of scatter which will be apparent in all of the figures and is probably caused primarily by experimental scatter. However, other unknown effects, such as free-stream turbulence, nonuniformities in free-stream flow, upstream history of wall-temperature gradients, and so forth, may contribute to the scatter. The possible error in obtaining an N value from the data may also contribute some scatter.

The solid line in figure 1(a) represents the conventional linear variation of N with $\log Re_{e,\theta}$ and has a slope m of approximately 2.0. Similar straight-line fairings can be

used to represent some of the data for other T_w/T_t ratios and other configurations. A summary of the resulting constants m and b in the equation

$$N = m \log R_{e,\theta} + b \quad (1)$$

are listed in table IV.

For $R_{e,\theta} > 10^4$, the "classical" behavior of an increase of N with an increase in $R_{e,\theta}$ is seen to occur for these data with no effect of Mach number. (See figs. 1(a) and 2.) In figures 1(a) and 1(b) for $R_{e,\theta} < 10^4$, the incompressible data show an increase in N from about 5 to 7 for $R_{e,\theta}$ from 10^3 to 10^4 , whereas the majority of the compressible supersonic data for $R_{e,\theta} < 10^4$ indicate a value of 6 to 7.5 for this range of $R_{e,\theta}$. The departure of the compressible data from the incompressible N values, shown in figures 1(a) and 1(b), indicates that there is an effect of Mach number upon N for $R_{e,\theta} < 10^4$. This effect is considered to be an indication of the "overshoot" as already defined. The data point in figure 1(a) of Ladenburg and Bershader from reference 34 (\triangleleft) with $N = 13.5$ was obtained close to transition ($(\Delta x)_{tr}/\delta \leq 0.1$); however, these data are subject to question because of the use of an interferometer in an extremely thin boundary layer ($\delta < 2$ mm).

Figure 1(c) shows that the values of N for $R_{e,\theta} < 10^4$ from some of the investigations actually increase to a peak and then decrease with increasing $R_{e,\theta}$ until values are more in line with the "classical" or conventional level for $R_{e,\theta} > 10^4$, where a gradual increase in N occurs with increasing $R_{e,\theta}$. The remaining data for $R_{e,\theta} > 10^4$ show a trend toward the conventional increase in N with increasing $R_{e,\theta}$, as depicted by the solid line in figure 1(c).

The variation of N with $R_{e,\theta}$ for $0.35 < T_w/T_t \leq 0.66$ is shown in figure 2 for the flat-plate class of flow, where again the overshoot is seen for $R_{e,\theta} < 10^4$. The data in figure 2 are for Mach numbers greater than 4.9 except for the data of references 53 (\triangle) and 56 (\blacktriangle). Comparison of the data in figures 1 and 2 shows that for the lower wall-to-total temperature ratio, somewhat lower values of N were obtained. The detailed variation of N with T_w/T_t will be considered in a subsequent section.

The variation of N with $R_{e,\theta}$ for the cold-wall data ($0.12 \leq T_w/T_t \leq 0.35$) is shown in figure 3. Again, some of the data exhibit an overshoot in N . All the data in figure 3 are for Mach numbers greater than 6.5 with the exception of the shock-tube data of Gooderum (ref. 55, \bullet) and Martin (ref. 56, \blacktriangle), which are at Mach numbers of 1.77 and 1.28, respectively. For a given value of $R_{e,\theta}$, the levels of N are reduced as the wall-to-total temperature ratio is reduced, as can be seen by a comparison of figures 1, 2, and 3.

N-Overshoot Phenomenon for Flat-Plate Class of Flows

From figures 1 to 3 for $Re_{e,\theta} < 10^4$, much of the experimental data for N overshoot the conventional incompressible variation. In addition to the incompressible data of figure 1(a), the incompressible transition data listed in reference 95 were examined in terms of the variation of N with $Re_{e,\theta}$ and were found to have no overshoot. The overshoot in N for the data in figures 2 and 3 is consistent with the results of figure 1(c). The majority of the data in figure 1(c) for $Re_{e,\theta} < 10^4$ are measured in a region where transition would ordinarily be considered as ended and the flow would be considered fully turbulent. From an examination of the data where the overshoot occurred, it was found that for these conditions ($Re_{e,\theta} < 10^4$) the values of skin friction and heat transfer seem to agree with turbulent boundary-layer flat-plate correlations and theory.

In order to ascertain if the large values of N for $Re_{e,\theta} < 10^4$ (termed the overshoot phenomena) were related to transition, the distance of the boundary-layer profile from the end of transition in terms of the boundary-layer thickness at the profile station was determined. The end of transition was determined from either data available in the reference or a correlation of transition Reynolds number with unit Reynolds numbers for various Mach numbers (ref. 96). The data in table I for the flat-plate class of flow were examined and, whenever possible, the parameter $(\Delta x)_{tr}/\delta$ was calculated; these values are listed in table I. For $Re_{e,\theta} < 10^4$, it was found that when $(\Delta x)_{tr}/\delta$ was small, the N values tended to be larger than the conventional values by a considerable amount.

Data from figure 1(c) in the overshoot region, which show an increase to a peak followed by a decrease in the values of N are shown by three groups of data:

(1) The data of Deem (refs. 20 and 21, \square) (top dashed line) were measured near the beginning of turbulent flow, which was determined from surface pitot measurements. The resulting values of $(\Delta x)_{tr}/\delta$ for these data were < 10 .

(2) The data of Sterrett and Emery (ref. 30, \triangleright) (middle dashed line) for $Me \approx 4.8$ on a flat plate had $(\Delta x)_{tr}/\delta$ values from 6 to 26.

(3) The data of Danberg in references 13 (\oplus), 14, and 15 (\triangle) (bottom dashed line) have values of $(\Delta x)_{tr}/\delta$ from < 1.0 to 19.

All of these data were obtained under untripped turbulent-flow conditions. The extremely high values of N found on a cone in helium (refs. 40 and 41, \triangleleft) may be due to an extreme overshoot phenomenon or may be characteristic of adiabatic helium boundary layers for high free-stream Mach numbers. (See fig. 1(c).) The relatively low level of free-stream turbulence and static pressure fluctuations (laminar side-wall boundary layer for an appreciable distance) may have caused the N overshoot found in the investigation of Korkegi (at $Me = 5.8$ ref. 29, \square) to remain at the level indicated, even though

$25 \leq (\Delta x)_{tr}/\delta \leq 34$. The fact that a turbulent boundary layer was difficult to obtain in reference 29 (large trips were necessary) may indicate that not only compressible flow but also a certain type of boundary-layer transition may be necessary before the data exhibit an overshoot trend.

The start of the overshoot in figure 3 begins with the Kutschenreuter et al. data of reference 19 (◆) at $N \approx 6.5$ for $Re_{e,\theta}$ of about 1800 ($(\Delta x)_{tr}/\delta \approx 2.3$) and rises to a maximum of $N \approx 10.0$ at an $Re_{e,\theta}$ of 2300. The cone data of Graber, Weber, and Softley (ref. 42, ▲) and of Softley and Sullivan (ref. 44, ▴) do not exhibit any overshoot for a $(\Delta x)_{tr}/\delta < 30$. The value of N for the cone profile from reference 44 (▴) appears to be exceptionally low. The reason for the lack of overshoot in these data is not known. Obviously, more data on cold-wall cones at $Me > 4$ need to be obtained before any firm conclusions can be drawn.

The effect of the variation of $(\Delta x)_{tr}/\delta$ on N is examined in figure 4(a) for the compressive data of figures 1(a) and 1(c) with $0.66 < T_w/T_t \leq 1.0$ and $Re_{e,\theta} < 8000$.

The unflagged data for the flat-plate and hollow cylinder show that as $(\Delta x)_{tr}/\delta$ increases the value of N generally decreases, with the most pronounced decrease in N occurring for $10 < (\Delta x)_{tr}/\delta < 60$. The flagged data for a cone or ogive cylinder, for $5 < (\Delta x)_{tr}/\delta < 90$, appear to have approximately the same slope as the unflagged data but the cone and ogive-cylinder data generally have higher values of N than the flat-plate data. These higher values are reasonable due to the fact that a cone boundary layer does not grow as rapidly as a flat-plate boundary layer, and hence longer relaxation distances are required. The unflagged flat-plate and hollow-cylinder data have a wide range of N values for $(\Delta x)_{tr}/\delta < 12$ due primarily to the scatter and the extreme overshoot in N near the end of transition, with the data near $(\Delta x)_{tr}/\delta \approx 0.1$ showing the largest overshoot values. A reasonable mean value for N from the flat-plate data used for $(\Delta x)_{tr}/\delta < 12$ would be approximately 10. For $12 \leq (\Delta x)_{tr}/\delta \leq 50$, the flat-plate class of flows in figure 4(a) appear to correlate as $N = 16.2 - 6.0 \log (\Delta x)_{tr}/\delta$. The cone and ogive-cylinder data for $5 < (\Delta x)_{tr}/\delta < 90$ correlate as $N = 20.5 - 6.0 \log (\Delta x)_{tr}/\delta$.

Figure 4(b) shows N plotted against $(\Delta x)_{tr}/\delta$ for the data from figures 2 and 3 for $Re_{e,\theta} < 8000$ and $0.1 \leq T_w/T_t \leq 0.66$. The $(\Delta x)_{tr}/\delta$ distance for much of the data in table I in this $Re_{e,\theta}$ and T_w/T_t range was either quite difficult to determine or could not be determined at all from the information that was available. This difficulty resulted in fewer $(\Delta x)_{tr}/\delta$ points in figure 4(b) than N data listed in table I and more scatter in the data of figure 4(b) than in those of figure 4(a). Within the scatter of the data for $0.35 < T_w/T_t \leq 0.66$ in figure 4(b), there appears to be a decrease in the value of N as $(\Delta x)_{tr}/\delta$ increases; however, there is no clear trend except that the bulk of the data for $(\Delta x)_{tr}/\delta < 40$ have N values between 8 and 10. The flagged data in figure 4(b) for

$0.12 \leq T_w/T_t \leq 0.35$ and $(\Delta x)_{tr}/\delta > 10.0$ may have low values of N due to the combined effects of the low wall-to-total temperature ratios and the relatively high values of $(\Delta x)_{tr}/\delta$.

It is possible that a correlation for N in terms of $(\Delta x)_{tr}/\delta$ could be obtained for the overshoot data ($(\Delta x)_{tr}/\delta < 50$), whereas a correlation in terms of $Re_{e,\theta}$ is better for data with $Re_{e,\theta} \geq 8000$. In general when the distance from the end of transition $(\Delta x)_{tr}/\delta$ was less than 30, the overshoot occurred. When $(\Delta x)_{tr}/\delta$ was greater than 30, there was little or no overshoot. Also, while there are insufficient data to ascertain a variation between N and Mach number for fixed $(\Delta x)_{tr}/\delta$, there is probably an effect of Mach number upon the degree of the overshoot. This effect is evidenced by the fact that the incompressible data of Schubauer and Klebanoff (ref. 58, A) show no overshoot, whereas the compressible data in the same range of $Re_{e,\theta}$ show an overshoot. (See figs. 1(a) and 1(b).) While in the present review all of the data have been taken at face value, it is interesting to speculate that the N overshoot near transition may be due, at least partially, to errors in pitot-probe measurements, which probably are larger near the end of transition than in fully turbulent flow. Near the end of transition, turbulence intensity has a peak, and this peak causes larger errors in pitot measurements. At higher Mach numbers, these errors are aggravated by increasingly larger density fluctuations; thus, at larger Mach numbers, larger overshoot occurs.

If the results of further investigations show that the large N overshoot (N greater than 7) seen in the data near transition is limited mainly to $M > 4.0$, speculation that the overshoot phenomenon may be related to the large amplification rates obtained from the second mode of linear instability theory may be made. (See fig. 10 of ref. 97.) This second mode first becomes dominant for $M > 4.0$, and the associated large amplification rates may trigger transition more abruptly to cause the observed increases in N . However, Morkovin points out (ref. 97) that on wind-tunnel models at hypersonic speeds the transition process may not be related to linear stability criteria because of the large free-stream disturbance levels usually present. These disturbances, which originate primarily in the tunnel-wall boundary layer, may cause transition to occur in a "high-intensity bypass mode" in which the linear theory does not play a part. Therefore, the overshoot could be due to a transition process dominated by the high-intensity bypass and might not occur for flight conditions where the large external disturbances are not present. More definitive data for $M > 4.0$ are needed to settle these questions.

Two-Dimensional Nozzle Walls

The velocity-profile N -power-law values for boundary layers on two-dimensional nozzle walls are shown in figures 5 and 6 for two of the same ranges of wall-to-total temperature ratios as shown for the flat-plate, cone, and hollow-cylinder data in

figures 1, 2, and 3. The majority of the data for two-dimensional nozzle walls are for $0.66 < T_w/T_t \leq 1.0$ and fall in the band indicated by the dashed lines in figure 5. For $Re_{e,\theta} < 20\,000$, this band ranges from $5.5 \leq N \leq 7.5$, while the band for $Re_{e,\theta} > 20\,000$ shows the usual increase in the value of N with an increase in the value of $Re_{e,\theta}$. The rise in the N value above the upper dashed line in figure 5 for $Re_{e,\theta} < 15\,000$ is similar to the overshoot trend found for flat-plate class of flows at $Re_{e,\theta} < 10^4$; however, available data indicate that the overshoot is most pronounced for flat plates, cones, and hollow cylinders at Mach numbers greater than 4.0 and near-adiabatic wall-to-total temperature ratios. In general, the Reynolds number in a nozzle-throat region is high enough so that transition should occur well upstream of the test-section measuring station, and no overshoot in N would be expected. However, in figure 5 the high N values from the data of Bell (ref. 69, Δ), Brinich (ref. 76, ∇), Matting et al. (ref. 70, \square), Ruptash (ref. 80, \triangleright), and the Aeromechanics Section of the Defense Research Laboratory (DRL) (ref. 78, ∇) are believed to be the result of transitional flow or the beginning of turbulent flow in the region just upstream of the profile measuring station.

Each of the five investigations mentioned were examined for any definite evidence, direct or indirect, that transition could be causing the N overshoot for $Re_{e,\theta} < 15\,000$. The conclusion for each of the five groups of data was that the proximity of transition was causing the N overshoot. The specific reasons for this finding for each investigation are as follows:

(1) In the investigation by Bell (ref. 69, Δ), the momentum thickness and the displacement thickness on the "flexible plate" for the Mach 4 and 5 tests showed a sudden increase as the unit Reynolds number increased. This sudden increase in the value of the boundary-layer integral thicknesses is indicative of transition, which could cause the observed overshoot in N . It is interesting to note that data obtained on the contoured wall have higher N values than the side-wall data for the same unit Reynolds number. These higher values are probably due to the longer region of favorable pressure gradient present at the contoured surface as compared with that at the side wall.

(2) The N data of Brinich (ref. 76, ∇) are similar to those of Bell (ref. 69, Δ) in that the bottom contoured wall gives higher values of N than the side wall for the same flow conditions. These higher values are again probably due to the longer region of favorable pressure gradient present at the contoured flow surface as noted.

(3) The low $Re_{e,\theta}$ datum point ($Re_{e,\theta} = 3620$) of Matting et al. (ref. 70, \square) at a value of $N = 9.8$ is in a region, where the flow is either transitional or just at the beginning of fully turbulent flow. From a plot of skin friction in reference 70, the datum point corresponding to this profile measurement falls in a region of skin-friction overshoot and is noted as being just slightly downstream of the end of transition.

(4) The data of Ruptash (ref. 80, \triangleright) show a sharply increasing value of N with increasing $Re_{e,\theta}$ from 4200 to 4700. The increase in $Re_{e,\theta}$ is a result of taking data at increasing x distances at a nominal Mach number of 3.0 for nearly constant stagnation conditions of $T_t = 83^\circ \text{ F}$ (301.6° K) and p_t of 1 atmosphere ($1.013 \times 10^5 \text{ N/m}^2$). The low stagnation pressure gives an $Re_{e,x}$ at the throat that is not large enough to produce transition based on flat-plate transition correlations extrapolated to Mach 1.0. In the test section the local $Re_{e,x}$ has increased above the flat-plate transition Reynolds number; therefore, it seems likely that transition has occurred upstream of the measuring station. The rise of the N values with increasing $Re_{e,\theta}$ (or $Re_{e,x}$) is characteristic of the rise to a peak of the overshoot data found in figure 1(c).

(5) The datum point of the Aeromechanics Section of DRL (ref. 78, ∇) at an $N = 8.2$ was measured in an extremely small nozzle (length from throat to exit of 5.29 inches (13.44 cm)) at a Reynolds number that was admitted by the author to be low. Although the tests were conducted with a tripping device just upstream of the throat, the flow at the measuring station was probably either transitional or barely turbulent.

The values of N for the moderately cool wall of a two-dimensional nozzle ($0.35 < T_w/T_t \leq 0.66$) from four investigations are shown in figure 6. The data exhibit a trend of increasing N with increasing $Re_{e,\theta}$.

Axisymmetric Nozzle Walls

The N values for axisymmetric nozzle walls are given in figures 7 and 8 for three ranges of wall-to-total temperature ratio. In figure 7 data are shown for $0.35 < T_w/T_t \leq 0.66$ and also for $0.94 \leq T_w/T_t \leq 1.0$. The single datum point at near-adiabatic wall conditions (at $N \approx 13$) is from an unpublished investigation by Watson (\triangleleft) made on the wall of the Langley 22-inch helium tunnel at a Mach number of 20.3. (All unpublished data presented in this paper were obtained at the Langley Research Center.) The value of θ in $Re_{e,\theta}$ for this helium datum point may be in error by a factor of ± 2.0 due to uncertainties in the measurement of the total temperature. This uncertainty factor represents the extremes of the values of $Re_{e,\theta}$ when either the values of the measured total temperature profile (obtained with an uncalibrated probe) or the assumption of a constant total temperature is used to reduce the data. The other data for $0.94 \leq T_w/T_t \leq 1.0$ in figure 7 are those of Tulin and Wright (ref. 90, \diamond), which were obtained upstream of the nozzle throat for the subsonic tests and in the Mach 1.19 test section of the Langley 8-foot high-speed tunnel for the supersonic tests. The data at $T_w/T_t \approx 0.94$ agree well with the high Mach number cold-wall axisymmetric nozzle data for $0.35 < T_w/T_t \leq 0.66$. The unpublished helium profiles of Watson (\triangleleft) show that the hypersonic helium turbulent boundary layers are characterized by extremely high values of

N in the turbulent outer part of the boundary layer and also by thick sublayers near the wall; this trend is also shown in references 40, 41, (\triangleleft), and 98. For values of $Re_{e,\theta} < 7000$, $0.35 < T_w/T_t \leq 0.66$, and Mach numbers greater than 6.0, the N values in figure 7 are approximately constant at 4.0 to 4.2, based mainly on the data of Hill (ref. 86, \diamond). For values of $Re_{e,\theta} > 7000$, the N data show the usual increase in N with an increase in $Re_{e,\theta}$. The solid line in figure 7 is essentially the same variation of N with $Re_{e,\theta}$ that was used in reference 10 except for a functional dependence on T_w/T_t .

The cold-wall ($0.12 \leq T_w/T_t \leq 0.35$) axisymmetric-nozzle data are shown in figure 8. In general, the data show no clear trend because of the scatter; however, as in the previous data, the average value of N is slightly lower than for the data at higher wall-temperature ratios. The flagged symbols in figure 8 indicate that the data were reduced by using the measured pitot pressures and an assumed temperature distribution through the boundary layer of $\frac{T_t - T_w}{T_{t,e} - T_w} = \left(\frac{u}{u_e}\right)^2$. It should be noted that the data of Perry and East (ref. 91, \triangleleft), Michel (ref. 87, \square), and Burke (ref. 88, \diamond) are for conical nozzles and the remaining data are for contoured nozzles. The large amount of scatter in figure 8 may be caused by a combination of the assumed temperature distribution used in references 87 and 88, and the fact that some of the nozzles are conical and some are contoured. When the data of figures 7 and 8 are combined (as was done in ref. 10), the overall trend of the data is similar to the curve with a $m = 5.0$ slope.

Comparison of N for the Three Configurations

In figure 9 is shown a comparison of the data of the flat plate, cone, and hollow cylinder, two-dimensional nozzle wall, and axisymmetric nozzle wall for $0.35 < T_w/T_t \leq 0.66$, which exhibit the conventional trend of an increase in N with an increase in $Re_{e,\theta}$; that is, for data at high $Re_{e,\theta}$, no overshoot occurs. Data with any overshoot effect found at the lower values of $Re_{e,\theta}$ (figs. 1 to 3) and the constant values of N found at low values of $Re_{e,\theta}$ (fig. 5) are not included in this figure. Both the data for the axisymmetric and two-dimensional nozzle walls in figure 9 increase with $Re_{e,\theta}$ at a slope of $m \approx 5.0$ (for a general equation of $N = m \log Re_{e,\theta} + b$), with the data of axisymmetric nozzle wall having higher values of N than those of the two-dimensional nozzle wall. At an $Re_{e,\theta} = 10^4$, the flat-plate, cone, and hollow-cylinder data coincide with the axisymmetric nozzle-wall data; however, the flat-plate, cone, and hollow-cylinder data have a slope of $m \approx 2$, which is considerably less than the slope for the nozzle-wall data.

The flat-plate, cone, and hollow-cylinder data and the two-dimensional nozzle-wall data in figure 1 ($0.66 < T_w/T_t \leq 1.35$) and figure 5 ($0.66 < T_w/T_t \leq 1.0$), respectively, are sufficiently numerous at $Re_{e,\theta} > 8000$ to indicate the slope of the conventional increase in N with $Re_{e,\theta}$.

VARIATION OF N WITH T_w/T_t FOR $M_e < 14.0$

The effect of wall temperature on the value of N has been investigated by plotting the variation of N with T_w/T_t for approximately constant values of $R_{e,\theta}$ as shown in figures 10 to 12. In general the relationship for N with a T_w/T_t variation included is

$$N = a \left(\frac{T_w}{T_t} \right)^c \quad (2)$$

where a is a function of $R_{e,\theta}$. The data in figure 10(a) for two-dimensional nozzle walls are for $R_{e,\theta} \approx 12\,500$ and $1.81 \leq M_e \leq 10.33$. For these data the exponent in the above relation is $c \approx 0.25$. Figure 10(b) is also for two-dimensional nozzle walls over about the same Mach number range but with $R_{e,\theta} \approx 20\,000$. Here the T_w/T_t exponent is also $c \approx 0.25$. The wall-temperature effect for axisymmetric nozzle-wall data is shown in figure 11 for $R_{e,\theta} \approx 2500$ and for $6.65 \leq M_e \leq 14.0$. Here again the slope of the data may be taken as $c \approx 0.25$. The wall-temperature effect on N for flat-plate data is shown in figure 12 for $R_{e,\theta} \approx 5000$, $T_w/T_t < 1.0$, and $1.77 \leq M_e \leq 5.8$. Two data points at $T_w/T_t = 1.35$ for $R_{e,\theta} = 3110$ and $R_{e,\theta} = 1940$ are included in this figure. The exponent of the wall-temperature ratio is again $c \approx 0.25$.

The results of figures 10 to 12 show that an increase in the wall-to-total temperature ratio varies the value of N by $c \approx 0.25$ at moderate Mach numbers. The apparent increase in N with an increase in wall-to-total temperature ratio shown in the tests of Higgins and Pappas (ref. 28, D) may be attributed partly to the proximity of the measuring station to the end of transition.

VARIATION OF N FOR HIGH MACH NUMBERS

The bulk of the data reviewed herein are for the $M < 12$ range, and, as stated previously, there is no discernible effect of Mach number upon N outside the overshoot region in this range. However, this may not be true at higher M values. Therefore, the use of the correlations given herein is not recommended for $M \gtrsim 14$.

A variation of N which might be applicable for the outer region of high Mach number ($M > 14$) turbulent boundary layers is described by the correlation of reference 98. The correlating parameter is ρ_e/ρ_w and is based largely on the high Mach number helium nozzle-wall boundary-layer data reported in reference 98. The only data reviewed herein which show a reasonable variation with this correlating parameter (ρ_e/ρ_w) are the helium nozzle-wall data of Watson, which have extremely low static temperatures resulting in large values of ρ_e/ρ_w . A comparison of the $M_e = 19.47$ nitrogen data of Clark and Harvey, presented in reference 10, at $T_w/T_t = 0.17$ with the unpublished $M_e = 20.3$ helium data of Watson at $T_w/T_t = 1.0$ is shown in figure 13. Although a

large difference in T_w/T_t and N ($N \approx 5.7$, ref. 10; $N = 13.25$, Watson) occurs for these two sets of data, the Mach number distributions appear to be similar. If it is assumed that the Mach number profile is invariant and has the form shown in figure 13

and that $\frac{T_t - T_w}{T_{t,e} - T_w} = \left(\frac{u}{u_e}\right)^2$ (ref. 10), then for high Mach numbers the velocity profile computed by using these two assumptions exhibit a large (almost 1st power) effect of T_w/T_t upon N .

CONCLUDING REMARKS

A survey of turbulent-boundary-layer velocity profiles with zero or slightly favorable pressure gradients has been made. For Mach numbers $\lesssim 14$, the following results were obtained:

Data for zero and slightly favorable pressure gradients were considered and classified according to three basic types of test configurations: (1) flat plate, cone, and hollow cylinder, (2) two-dimensional nozzle walls, and (3) axisymmetric nozzle walls. The data were plotted for each configuration against $Re_{e,\theta}$ for three ranges of wall-to-total temperature ratios T_w/T_t : (1) $0.66 < T_w/T_t \leq 1.35$; (2) $0.35 < T_w/T_t \leq 0.66$; and (3) $0.12 \leq T_w/T_t \leq 0.35$.

It was found that when the survey station was in the region of the beginning of turbulent flow ($Re_{e,\theta}$ less than approximately 8000), there was generally an "overshoot" in the values of N . The available data indicate that the overshoot is most pronounced for flat plates, cones, and hollow cylinders at Mach numbers greater than 4.0 and near-adiabatic wall-to-total temperature ratios. In general, when the ratio of the distance from the end of transition $(\Delta x)_{tr}$ to the boundary-layer thickness δ was less than 30, the overshoot occurred; and when $(\Delta x)_{tr}/\delta$ was greater than 30, there was no overshoot. The available data indicate that an N overshoot may occur for nozzle walls when conditions such as a short nozzle or low unit Reynolds number cause transition to take place in the downstream part of the nozzle so that the boundary layer at the measuring station is either transitional or just fully turbulent.

When $Re_{e,\theta}$ is large enough to avoid overshoot in the N values, there is an increase in N with an increase in $Re_{e,\theta}$, with a trend and level similar to incompressible data. The data for two-dimensional and axisymmetric nozzle walls indicate a slope for the conventional variation of $m \approx 5$. The flat-plate class of data have a slope of $m \approx 2.0$.

The wall-temperature effect for all three configurations shows an increase in N with an increase in T_w/T_t at nearly constant values of Re_{θ} . The slope c of the wall-temperature effect is approximately 0.25 for N proportional to $(T_w/T_t)^c$ with Re_{θ} constant.

Langley Research Center,

National Aeronautics and Space Administration,

Langley Station, Hampton, Va., January 23, 1970.

REFERENCES

1. Schlichting, Hermann (J. Kestin, trans.): *Boundary Layer Theory*. Fourth ed., McGraw-Hill Book Co., Inc., c.1960.
2. Thompson, B. G. J.: *A Critical Review of Existing Methods of Calculating the Turbulent Boundary Layer*. *Brit. A.R.C.* 26 109, Aug. 7, 1964.
3. Sibulkin, Merwin: *Heat Transfer to an Incompressible Turbulent Boundary Layer and Estimation of Heat-Transfer Coefficients at Supersonic Nozzle Throats*. *J. Aeronaut. Sci.*, vol. 23, no. 2, Feb. 1956, pp. 162-172.
4. Elliott, David G.; Bartz, Donald R.; and Silver, Sidney: *Calculation of Turbulent Boundary-Layer Growth and Heat Transfer in Axisymmetric Nozzles*. Tech. Rep. No. 32-387 (Contract No. NAS 7-100), Jet Propulsion Lab., California Inst. Technol., Feb. 15, 1963.
5. Pinckney, S. Z.: *Static-Temperature Distribution in a Flat-Plate Compressible Turbulent Boundary Layer With Heat Transfer*. NASA TN D-4611, 1968.
6. Persh, Jerome; and Lee, Roland: *A Method for Calculating Turbulent Boundary Layer Development in Supersonic and Hypersonic Nozzles Including the Effects of Heat Transfer*. NAVORD Rep. 4200 (Aeroballistic Res. Rep. 320), U.S. Navy, June 7, 1956.
7. Enkenhus, K. R.; and Maher, E. F.: *The Aerodynamic Design of Axisymmetric Nozzles for High-Temperature Air*. NAVWEPS Rep. 7395, U.S. Navy, Feb. 5, 1962.
8. Miller, Leonard D.: *Predicting Turbulent Compressible Boundary Layers in Strong Adverse Pressure Gradients*. AIAA Paper No. 67-196, Jan. 1967.
9. Scaggs, Norman E.: *Boundary Layer Profile Measurements in Hypersonic Nozzles*. ARL 66-0141, U.S. Air Force, July 1966.
10. Bushnell, Dennis M.; Johnson, Charles B.; Harvey, William D.; and Feller, William V.: *Comparison of Prediction Methods and Studies of Relaxation in Hypersonic Turbulent Nozzle-Wall Boundary Layers*. NASA TN D-5433, 1969.
11. Shutts, W. H.; Hartwig, W. H.; and Weiler, J. E.: *Final Report on Turbulent Boundary-Layer and Skin-Friction Measurements on a Smooth, Thermally Insulated Flat Plate at Supersonic Speeds*. DRL-364, CM-823 (Contract NOrd-9195), Univ. of Texas, Jan. 5, 1955.
12. Coles, Donald: *Measurements in the Boundary Layer on a Smooth Flat Plate in Supersonic Flow - III. Measurements in a Flat-Plate Boundary Layer at the Jet Propulsion Laboratory*. Rep. No. 20-71 (Contract No. DA-04-495-Ord 18), Jet Propulsion Lab., California Inst. Technol., June 1, 1953.

13. Danberg, James E.: Measurement of the Characteristics of the Compressible Turbulent Boundary Layer With Air Injection. NAVORD Rep. 6683, U.S. Navy, Sept. 3, 1959.
14. Danberg, James E.: Characteristics of the Turbulent Boundary Layer With Heat and Mass Transfer: Data Tabulation. NOLTR-67-6, U.S. Navy, Jan. 23, 1967. (Available from DDC as AD 650 272.)
15. Danberg, James E.: Characteristics of the Turbulent Boundary Layer With Heat and Mass Transfer at $M=6.7$. NOLTR 64-99, U.S. Navy, Oct. 19, 1964.
16. Winkler, Eva M.; and Cha, Moon H.: Investigation of Flat Plate Hypersonic Turbulent Boundary Layers With Heat Transfer at a Mach Number of 5.2. NAVORD Rep. 6631, U.S. Navy, Sept. 15, 1959.
17. Pinckney, S. Z.: Data on Effects of Incident-Reflecting Shocks on the Turbulent Boundary Layer. NASA TM X-1221, 1966.
18. Wilson, R. E.: Characteristics of Turbulent Boundary Layer Flow Over a Smooth, Thermally Insulated Flat Plate at Supersonic Speeds. DRL-301, CM-712 (Contract NOrd-9195), Univ. of Texas, June 1, 1952.
19. Kutschenreuter, Paul H., Jr.; Brown, David L.; Hoelmer, Werner; et al.: Investigation of Hypersonic Inlet Shock-Wave Boundary Layer Interaction. Part II - Continuous Flow Test and Analyses. AFFDL-TR-65-36, U.S. Air Force, Apr. 1966.
20. Deem, R. E.: Results of a Flat Plate Boundary Layer Transition Experiment at Mach 5 - Model: General. Rep. No. SM-47643 (Contract No. AF 33(657)-10660), Missile & Space Syst. Div., Douglas Aircraft Co., June 10, 1964.
21. Deem, R. E.: Results of a Flat Plate Boundary Layer Transition Experiment at Mach 8 - Model: General. Rep. No. SM-45918 (Contract No. AF 33(657)-10660), Missile & Space Syst. Div., Douglas Aircraft Co., Apr. 24, 1964. (Available from DDC as AD 805 547.)
22. Deem, R. E.: Results of a Flat Plate Boundary Layer Transition Experiment at Mach 10 - Model: General. Rep. No. SM-47630 (Contract No. AF 33(657)-10660), Missile & Space Syst. Div., Douglas Aircraft Co., May 22, 1964.
23. Seddon, J.: The Flow Produced by Interaction of a Turbulent Boundary Layer With a Normal Shock Wave of Strength Sufficient to Cause Separation. R. & M. No. 3502, Brit. A.R.C., 1967.
24. Hakkinen, Raimo J.: Measurements of Turbulent Skin Friction on a Flat Plate at Transonic Speeds. NACA TN 3486, 1955.

25. Hopkins, Edward J.; Rubesin, Morris W.; Inouye, Mamoru; Keener, Earl R.; Mateer, George C.; and Polek, Thomas E.: Summary and Correlation of Skin-Friction and Heat-Transfer Data for a Hypersonic Turbulent Boundary Layer on Simple Shapes. NASA TN D-5089, 1969.
26. Morrisette, E. Leon; Stone, David R.; and Cary, Aubrey M., Jr.: Downstream Effects of Boundary-Layer Trips in Hypersonic Flow. Compressible Turbulent Boundary Layers, NASA SP-216, 1969, pp. 437-453.
27. Wagner, R. D., Jr.; Maddalon, D. V.; Weinstein, L. M.; and Henderson, A., Jr.: Influence of Measured Free-Stream Disturbances on Hypersonic Boundary-Layer Transition. AIAA Pap. No. 69-704, June 1969.
28. Higgins, Robert W.; and Pappas, Constantine C.: An Experimental Investigation of the Effect of Surface Heating on Boundary-Layer Transition on a Flat Plate in Supersonic Flow. NACA TN 2351, 1951.
29. Korkegi, R. H.: Transition Studies and Skin Friction Measurements on an Insulated Flat Plate at a Hypersonic Mach Number. Memo. No. 17 (Contract No. DA-04-495-Ord-19), GALCIT, July 15, 1954.
30. Sterrett, James R.; and Emery, James C.: Extension of Boundary-Layer-Separation Criteria to a Mach Number of 6.5 By Utilizing Flat Plates With Forward-Facing Steps. NASA TN D-618, 1960.
31. Moore, Dave R.: Velocity Similarity in the Compressible Turbulent Boundary Layer With Heat Transfer. Ph. D. Dissertation, Univ. of Texas, 1962.
32. Richards, Bryan E.: Transitional and Turbulent Boundary Layers on a Cold Flat Plate in Hypersonic Flow. Aeronaut. Quart., vol. XVIII, pt. 3, Aug. 1967, pp. 237-257.
33. Monaghan, R. J.; and Cooke, J. R.: The Measurement of Heat Transfer and Skin Friction at Supersonic Speeds. Part IV - Tests on a Flat Plate at $M = 2.82$. C.P. No. 140, Brit. A.R.C., 1953.
34. Ladenburg, R.; and Bershader, D.: Optical Studies of Boundary Layer Phenomena on a Flat Plate at Mach Number 2.35. NR061-020 (Contract N6ori-105, Task II), Dep. Phys., Princeton Univ., Dec. 15, 1952.
35. Woodruff, Lawrence W.; and Lorenz, George C.: Hypersonic Turbulent Transpiration Cooling Including Downstream Effects. AIAA J., vol. 4, no. 6, June 1966, pp. 969-975.
36. Nothwang, George J.: An Evaluation of Four Experimental Methods for Measuring Mean Properties of a Supersonic Turbulent Boundary Layer. NACA Rep. 1320, 1957. (Supersedes NACA TN 3721.)

37. Moore, D. R.; and Harkness, J.: Experimental Investigations of the Compressible Turbulent Boundary Layer at Very High Reynolds Numbers. AIAA J., vol. 3, no. 4, Apr. 1965, pp. 631-638.
38. Allen, Jerry M.; and Monta, William J.: Turbulent-Boundary-Layer Characteristics of Pointed Slender Bodies of Revolution at Supersonic Speeds. NASA TN D-4193, 1967.
39. Bradfield, Walter S.: An Experimental Investigation of the Turbulent Boundary Layer in Supersonic Flow Around Unyawed Cones With Small Heat Transfer and Correlations With Two Dimensional Data. Res. Rep. No. 1, Convair Sci., Res. Lab., Mar. 15, 1958.
40. Maddalon, Dal V.; and Henderson, Arthur, Jr.: Boundary-Layer Transition on Sharp Cones at Hypersonic Mach Numbers. AIAA J., vol. 6, no. 3, Mar. 1968, pp. 424-431.
41. Henderson, A.; Rogallo, R. S.; Woods, W. C.; and Spitzer, C. R.: Exploratory Hypersonic Boundary-Layer Transition Studies. AIAA J. (Tech Notes), vol. 3, no. 7, July 1965, pp. 1363-1364.
42. Graber, B. C.; Weber, H. E.; and Softley, E. J.: Comparison of Laminar and Turbulent Cone Boundary Layer Flow With and Without Pressure Gradient. R67SD49, Missile Space Div., Gen. Elec. Co., Nov. 1967.
43. Martellucci, A.; Rie, H.; and Sontowski, J. F.: Evaluation of Several Eddy Viscosity Models Through Comparison With Measurements in Hypersonic Flows. AGARD CP No. 30, May 1968, pp. 3-1 - 3-18.
44. Softley, Eric J.; and Sullivan, Robert J.: Theory and Experiment for the Structure of Some Hypersonic Boundary Layers. Presented at AGARD Specialists Meeting on Hypersonic Boundary Layers and Flow Fields (London, England), May 1-3, 1968.
45. Bradfield, W. S.; DeCoursin, D. G.; and Blumer, C. B.: Characteristics of Laminar and Turbulent Boundary Layer at Supersonic Velocity. Rep. No. 83, Rosemount Aero. Labs., Univ. Minn. Inst. Tech., July 1952.
46. Adcock, Jerry B.; Peterson, John B., Jr.; and McRee, Donald I.: Experimental Investigation of a Turbulent Boundary Layer at Mach 6, High Reynolds Numbers, and Zero Heat Transfer. NASA TN D-2907, 1965.
47. Stroud, J. F.; and Miller, L. D.: An Experimental and Analytical Investigation of Hypersonic Inlet Boundary Layers. Volume II. Data Reduction Program and Tabulated Experimental Data. AFFDL-TR-65-123 - Vol. II, U.S. Air Force, Aug. 1965. (Available from DDC as AD 621 344.)

48. Samuels, Richard D.; Peterson, John B., Jr.; and Adcock, Jerry B.: Experimental Investigation of the Turbulent Boundary Layer at a Mach Number of 6 With Heat Transfer at High Reynolds Numbers. NASA TN D-3858, 1967.
49. O'Donnell, Robert M.: Experimental Investigation at a Mach Number of 2.41 of Average Skin-Friction Coefficients and Velocity Profiles for Laminar and Turbulent Boundary Layers and an Assessment of Probe Effects. NACA TN 3122, 1954.
50. Brinich, Paul F.; and Diaconis, Nick S.: Boundary-Layer Development and Skin Friction at Mach Number 3.05. NACA TN 2742, 1952.
51. Hoydysh, Walter G.; and Zakkay, Victor: An Experimental Investigation of Hypersonic Turbulent Boundary Layers in Adverse Pressure Gradient. Rep. No. F-67-5, New York Univ., Aug. 1967.
52. Aircraft Div., Douglas Aircraft Co., Inc.: Investigation of Skin Friction Drag on Practical Construction Surfaces for the Supersonic Transport. FDL TDR 64-74, U.S. Air Force, Aug. 1964.
53. Swanson, Andrew G.; Buglia, James J.; and Chauvin, Leo T.: Flight Measurements of Boundary-Layer Temperature Profiles on a Body of Revolution (NACA RM-10) at Mach Numbers From 1.2 to 3.5. NACA TN 4061, 1957.
54. Jones, Robert A.; and Feller, William V.: Preliminary Surveys of the Wall Boundary Layer in a Mach 6 Axisymmetric Tunnel. NASA TN D-5620, 1970.
55. Gooderum, Paul B.: An Experimental Study of the Turbulent Boundary Layer on a Shock-Tube Wall. NACA TN 4243, 1958.
56. Martin, Walter A.: An Experimental Study of the Turbulent Boundary Layer Behind the Initial Shock Wave in a Shock Tube. Aero/Space Sci., vol. 25, no. 10, Oct. 1958, pp. 644-652.
57. Chapman, Dean R.; and Kester, Robert H.: Turbulent Boundary-Layer and Skin-Friction Measurements in Axial Flow Along Cylinders at Mach Numbers Between 0.5 and 3.6. NACA TN 3097, 1954.
58. Schubauer, G. B.; and Klebanoff, P. S.: Contributions of the Mechanics of Boundary-Layer Transition. NACA Rep. 1289, 1956. (Supersedes NACA TN 3489.)
59. Patel, V. C.; and Head, M. R.: Reversion of Turbulent to Laminar Flow. J. Fluid Mech., vol. 34, pt. 2, Nov. 12, 1968, pp. 371-392.
60. Wooldridge, C. E.; and Willmarth, W. W.: Measurements of the Correlation Between the Fluctuating Velocities and the Fluctuating Wall Pressure in a Thick Turbulent Boundary Layer. 02920-2-T (Contract No. Nonr-1224(30)), College Eng., Univ. of Michigan, Apr. 1962.

61. Favre, A. J.; Gaviglio, J. J.; and Dumas, R.: Space-Time Double Correlations and Spectra in a Turbulent Boundary Layer. *J. Fluid Mech.*, vol. 2, pt. 4, June 1957, pp. 313-342.
62. Ross, Donald: A Study of Incompressible Turbulent Boundary Layers. Ph. D. Thesis, Harvard Univ., 1953.
63. van der Hegge Zijnen, B. G.: Measurements of the Velocity Distribution in the Boundary Layer Along a Plane Surface. Rep. 6, Aero. Lab. Tech. H. S. Delft, 1924.
64. Bertram, Mitchel H.; and Neal, Luther, Jr.: Recent Experiments in Hypersonic Turbulent Boundary Layers. Presented at the AGARD Specialists' Meeting on Recent Developments in Boundary-Layer Research (Naples, Italy), May 10-14, 1965.
65. Lobb, R. Kenneth; Winkler, Eva M.; and Persh, Jerome: NOL Hypersonic Tunnel No. 4 Results VII: Experimental Investigation of Turbulent Boundary Layers in Hypersonic Flow. NAVORD Rep. 3880, U.S. Navy, Mar. 1, 1955.
66. Spivack, H. M.: Experiments in the Turbulent Boundary Layer of a Supersonic Flow. Rep. No. CM-615, N. Amer. Aviat., Inc., Jan. 16, 1950.
67. Bartle, E. Roy; and Leadon, Bernard M.: The Compressible Turbulent Boundary Layer on a Flat Plate With Transpiration Cooling – I. Measurements of Heat Transfer and Boundary Layer Profiles. Res. Rep. No. 11, Convair Sci. Res. Lab., May 1961.
68. Jeromin, L. O. F.: An Experimental Investigation of the Compressible Turbulent Boundary Layer With Air Injection. R. & M. No. 3526, Brit. A.R.C., 1968.
69. Bell, D. R.: Boundary-Layer Characteristics at Mach Numbers 2 Through 5 in the Test Section of the 12-Inch Supersonic Tunnel (D). AEDC-TDR-63-192, U.S. Air Force, Sept. 1963.
70. Matting, Fred W.; Chapman, Dean R.; Nyholm, Jack R.; and Thomas, Andrew G.: Turbulent Skin Friction at High Mach Numbers and Reynolds Numbers in Air and Helium. NASA TR R-82, 1961.
71. Kistler, Alan L.: Fluctuation Measurements in a Supersonic Turbulent Boundary Layer. *Phys. Fluids*, vol. 2, no. 3, May-June 1959, pp. 290-296.
72. Lee, Roland E.; Yanta, William J.; and Leonas, Annette C.: Velocity Profile, Skin Friction Balance and Heat Transfer Measurements of the Turbulent Boundary Layer at Mach 5. Proceedings of the 1968 Heat Transfer and Fluid Mechanics Institute, Ashley F. Emery and Creighton A. Depew, eds., Stanford Univ. Press, c.1968.

73. Kepler, C. E.; and O'Brien, R. L.: Supersonic Turbulent Boundary Layer Growth Over Cooled Walls in Adverse Pressure Gradients. ASD-TDR-62-87, U.S. Air Force, Oct. 1962.
74. Baron, Judson R.: Analytic Design of a Family of Supersonic Nozzles by the Friedrichs Method, Including Computation Tables and a Summary of Calibration Data. WADC Tech. Rep. 54-279, U.S. Air Force, June 1954.
75. Jackson, Mary W.; Czarnecki, K. R.; and Monta, William J.: Turbulent Skin Friction at High Reynolds Numbers and Low Supersonic Velocities. NASA TN D-2687, 1965.
76. Brinich, Paul F.: Boundary-Layer Measurements in 3.84- by 10-inch Supersonic Channel. NACA TN 2203, 1950.
77. Speaker, W. V.; and Ailman, C. M.: Spectra and Space-Time Correlations of the Fluctuating Pressures at a Wall Beneath a Supersonic Turbulent Boundary Layer Perturbed by Steps and Shock Waves. NASA CR-486, 1966.
78. Aeromechanics Sec.: Aerodynamic Characteristics of Nozzles and Diffusers for Supersonic Wind Tunnels. DRL-281 (Contract AF 33(038)-10112), Univ. of Texas, Apr. 27, 1951.
79. Winter, K. G.; Smith, K. G.; and Gaudet, L.: Measurements of Turbulent Skin Friction at High Reynolds Numbers at Mach Numbers of 0.2 and 2.2. Recent Developments in Boundary Layer Research, Pt. I, AGARDograph 97, May 1965, pp. 97-123.
80. Ruptash, J.: Boundary Layer Measurements in the UTIA 5- by 7-Inch Supersonic Wind Tunnel. Rep. No. 16, Inst. Aerophys., Univ. of Toronto, May 1952.
81. Thomann, Hansheiri: Messung von Wärmeübergang und Eigentemperatur in Turbulenter Grenzschicht bei $M = 1,81$ und $2,02$ (Measurement of Heat Transmission and Temperature in a Turbulent Boundary Layer Between $M = 1.81$ and 2.02). SE-75:1, Flygtekniska Försöksanstalten, 1957.
82. Jones, Jerry: An Investigation of the Boundary-Layer Characteristics in the Test Section of a 40 by 40-Inch Supersonic Tunnel. AEDC-TN-60-189, U.S. Air Force, Oct. 1960.
83. Dershin, H.; Leonard, C. A.; Gallaher, W. H.; and Palmer, J. P.: Direct Measurement of Compressible, Turbulent Boundary Layer Skin Friction on a Porous Flat Plate With Mass Injection. NASA CR-79095, 1966.
84. Meier, Hans Ulrich: Measurements of Turbulent Boundary Layers on a Heat-Insulated Wall in the Small Supersonic Wind Tunnel of the AVA. NASA TT F-12 547, 1969.

85. Thomke, G. J.; and Roshko, A.: Incipient Separation of a Turbulent Boundary Layer at High Reynolds Number in Two-Dimensional Supersonic Flow Over a Compression Corner. NASA CR-73308, 1969.
86. Hill, F. K.: Turbulent Boundary Layer Measurements at Mach Numbers From 8 to 10. Phys. Fluids, vol. 2, no. 6, Nov.-Dec. 1959, pp. 668-680.
87. Michel, R.: Developpement de la Couche Limite Dans Une Tuyere Hypersonique. The High Temperature Aspects of Hypersonic Flow, Wilbur C. Nelson, ed., Pergamon Press, c.1964, pp. 693-719.
88. Burke, Andrew F.: Turbulent Boundary Layers on Highly Cooled Surfaces at High Mach Numbers. Proceedings of Symposium on Aerothermoelasticity, ASD Tech. Rep. 61-645, U.S. Air Force, 1961, pp. 704-741.
89. Shall, Paul Joseph, Jr.: A Boundary Layer Study on Hypersonic Nozzles. M.S. Thesis, U.S. Air Force Institute of Technology, Mar. 1968. (Available from DDC as AD 833 236.)
90. Tulin, Marshall P.; and Wright, Ray H.: Investigation of Some Turbulent-Boundary-Layer Velocity Profiles at a Tunnel Wall With Mach Numbers up to 1.2. NACA RM L9H29a, 1949.
91. Perry, J. H.; and East, R. A.: Experimental Measurements of Cold Wall Turbulent Hypersonic Boundary Layers. AGARD CP No. 30, May 1968, pp. 2-1 - 2-19.
92. Matthews, R. K.; and Trimmer, L. L.: Nozzle Turbulent Boundary-Layer Measurements in the VKF 50-In. Hypersonic Tunnels. AEDC-TR-69-118, U.S. Air Force, June 1969.
93. Banner, L. T.; and Williams, M. J.: Boundary Layer Measurements in the A.R.L. Hypersonic Tunnel Conical Nozzle. Note ARL/Aero. 215, Aust. Def. Sci. Serv., July 1963.
94. Persh, Jerome: A Theoretical Investigation of Turbulent Boundary Layer Flow With Heat Transfer at Supersonic and Hypersonic Speeds. NAVORD Rep. 3854, U.S. Navy, May 19, 1955.
95. Persh, Jerome: A Study of Boundary-Layer Transition From Laminar to Turbulent Flow. NAVORD Rep. 4339, U.S. Navy, Nov. 21, 1956.
96. Stainback, P. Calvin (With appendix by P. Calvin Stainback and Kathleen C. Wicker): Effect of Unit Reynolds Number, Nose Bluntness, Angle of Attack, and Roughness on Transition on a 5° Half-Angle Cone at Mach 8. NASA TN D-4961, 1969.

97. Morkovin, Mark V.: Critical Evaluation of Transition From Laminar to Turbulent Shear Layers With Emphasis on Hypersonically Traveling Bodies. AFFDL-TR-68-149, U.S. Air Force, Mar. 1969. (Available from DDC as AD 686 178.)
98. Kemp, Joseph H., Jr.; and Sreekanth, A. K.: Preliminary Results From an Experimental Investigation of Nozzle Wall Boundary Layers at Mach Numbers Ranging From 27 to 47. AIAA Paper No. 69-686, June 1969.

TABLE I.- KEY FOR TURBULENT-BOUNDARY-LAYER DATA FOR FLAT PLATE
AND AXISYMMETRIC BODIES

(a) Compressible data

Symbol	Reference		$Re_{e,\theta}$	θ , mm	M_e	T_w/T_t	N	$\frac{(\Delta x)_{tr}}{\delta}$	Transition
	Number	Author							
Flat plate									
◩	a ¹¹	Shutts, Hartwig and Weiler	0.608×10^4	0.277	1.73	0.958	6.23	70	Tripped ↓
			1.165	.523	1.73	.958	7.27	74	
			1.984	.889	1.73	.958	7.98	77	
			1.615	.653	2.00	.952	8.58	79	
◊	12	Coles	0.498×10^4	0.394	4.54	0.956	6.36	61	Tripped ↓
			.659	.526	4.55	.955	6.03	50	
			.347	.538	4.51	.955	5.68	50	
			.756	.569	3.70	.944	5.47	54	
			.410	.632	3.70	.943	5.92	43	
			.212	.559	3.69	.933	6.59	50	
			1.020	.668	2.58	.927	5.88	57	
			.660	.744	2.57	.923	6.68	52	
			.219	.709	2.54	.923	5.46	58	
			.857	.767	1.98	.919	5.53	61	
			.647	.815	1.98	.918	5.45	56	
			.298	.945	1.97	.918	5.63	46	
⊠	13	Danberg	0.351×10^4	0.242	5.05	0.833	7.86	<1	Untripped ↓
			.319	.214	5.09	.745	8.24	<1	
			.400	.265	5.18	.818	7.60	<1	
			.401	.268	5.20	.721	7.91	<1	
⊠	14 and 15	Danberg	0.253×10^4	0.312	6.54	0.481	8.31	11	Untripped ↓
			.303	.382	6.49	.476	7.85	15	
			.235	.306	6.44	.469	8.78	10	
			.302	.306	6.45	.460	8.34	13	
			.267	.303	6.45	.582	8.00	15	
			.132	.176	6.31	.850	8.38	<1	
			.172	.215	6.45	.830	8.70	4	
			.220	.248	6.61	.831	8.78	10	
			.284	.314	6.62	.822	8.90	13	
			.286	.280	6.43	.840	8.70	11	
			.490	.265	6.34	.783	7.84	19	
.252	.287	6.62	.587	8.70	10				
△	a ¹⁶	Winkler and Cha	0.210×10^4	0.616	5.14	0.802	9.9	<0.1	Untripped ↓
			.294	.189	5.14	.877	10.0	<.1	
			.317	.228	5.20	.838	9.3	7	
			.388	.284	5.26	.844	8.2	18	
			.430	.322	5.29	.844	7.0	24	
			.190	.179	4.98	.757	9.7	<.1	
			.178	.149	5.18	.742	11.2	<.1	
			.296	.227	5.20	.752	9.9	6	

^aValue of N obtained directly from report and not from replot of velocity profile.

TABLE I.- KEY FOR TURBULENT-BOUNDARY-LAYER DATA FOR FLAT PLATE
AND AXISYMMETRIC BODIES - Continued

(a) Compressible data - Continued

Symbol	Reference		$Re_{e,\theta}$	θ , mm	Me	T_w/T_t	N	$\frac{(\Delta x)_{tr}}{\delta}$	Transition
	Number	Author							
Flat plate									
△	a16	Winkler and Cha	0.345×10^4	0.280	5.24	0.759	8.0	16	Untripped ↓ ↓ ↓ ↓ ↓ ↓ ↓ ↓ ↓
			.379	.330	5.24	.766	6.7	25	
			.105	.114	5.17	.613	6.9	<.1	
			.165	.188	5.16	.586	9.5	9	
			.173	.186	5.10	.578	10.3	8	
			.248	.281	5.24	.589	9.8	17	
			.240	.256	5.11	.564	9.1	18	
			.326	.343	5.12	.604	8.7	22	
			◇	17	Pinckney	1.699×10^4	0.625	1.99	
1.920	.358	4.24				.928	7.67	57.3	
2.825	.383	4.16				.930	8.60	51.4	
4.500	.764	4.15				.970	9.86	54.0	
2.958	1.031	3.02				.956	8.26	---	
4.435	1.123	3.05				.955	8.80	---	
5.465	1.034	3.04				.960	9.07	---	
4.048	1.239	2.33				.944	9.36	---	
4.920	1.554	2.31				.954	8.78	---	
5.180	1.300	2.27				.942	9.32	---	
○	a18	Wilson	0.453×10^4	0.178	2.00	0.952	6.3	70	Untripped ↓ ↓ ↓ ↓ ↓ ↓ ↓ ↓ ↓ ↓ ↓ ↓ ↓ ↓ ↓ ↓
			.695	.272	2.00	.952	7.1	48	
			1.220	.480	2.00	.952	7.4	66	
			1.510	.589	2.00	.952	7.5	60	
			1.730	.678	2.00	.952	7.8	60	
			.605	.264	1.73	.958	6.4	---	
			1.090	.477	1.73	.958	6.8	---	
			1.320	.579	1.73	.958	7.0	---	
			1.260	.551	1.73	.958	6.8	---	
			1.476	.645	1.73	.958	8.0	---	
			1.696	.749	1.73	.958	7.7	---	
			1.886	.836	1.73	.958	8.2	---	
			.518	.216	2.50	.940	6.4	60	
			.762	.323	2.50	.940	6.7	66	
			.957	.409	2.50	.940	7.0	70	
			1.218	.513	2.50	.940	7.0	72	
			1.535	.648	2.50	.940	6.7	63	
1.660	.686	2.50	.940	7.5	65				
1.834	.759	2.50	.940	7.9	68				
1.840	.762	2.50	.940	7.6	68				
1.560	.648	2.50	.940	7.7	---				

^aValue of N obtained directly from report and not from replot of velocity profile.

TABLE I.- KEY FOR TURBULENT-BOUNDARY-LAYER DATA FOR FLAT PLATE
AND AXISYMMETRIC BODIES - Continued

(a) Compressible data - Continued

Symbol	Reference		Re_{θ}	θ , mm	Me	T_w/T_t	N	$\frac{(\Delta x)_{tr}}{\delta}$	Transition	
	Number	Author								
Flat plate										
◆	19	Kutschenreuter et al.	0.179×10^4	0.239	9.00	0.300	6.56	----	Untripped	
			.199	.231	9.01	.300	6.22	----	Untripped	
			.229	.299	8.97	.306	10.0	----	Tripped	
			.210	.197	9.00	.295	9.30	2.3	Tripped	
			.347	.322	6.60	.397	8.34	----	Untripped	
			.486	.447	6.50	.397	7.95	----	Untripped	
			.332	.269	6.54	.437	8.14	----	Tripped	
			.445	.422	6.58	.437	7.42	----	Untripped	
			.636	.538	6.55	.410	6.96	----	Tripped	
			.576	.533	6.55	.390	6.82	----	Untripped	
◊	20, 21, and 22	Deem	0.301×10^4	0.442	9.83	0.564	12.9	<5	Untripped	
			.301	.251	7.84	.800	11.8	<5	↓	
			.382	.330	7.83	.797	11.0	<5		
			.203	.305	7.87	.819	9.75	<5		
			.240	.259	7.85	.803	11.2	<5		
			.218	.170	5.11	.909	9.75	<4		
			.251	.112	4.96	.902	11.70	<5		
			.213	.292	5.07	.912	9.1	<7		
			.319	.190	4.96	.893	9.2	<7		
			.269	.693	3.01	.882	6.4	<10		
⊠	23	Seddon	0.385×10^4	0.391	1.47	0.969	5.8	56		Tripped
◻	24	Hakkinen	0.191×10^4	0.143	1.48	0.968	5.2	43	Tripped	
■	^a 25	Hopkins et al.	0.219×10^4	0.394	6.5	0.308	9.5	----	Untripped	
.456			.531	6.5	.300	9.7	----	Tripped		
.330			.612	6.5	.391	8.7	----	Tripped		
.382			.411	6.5	.408	9.4	33	Untripped		
.833			.630	6.5	.465	7.3	----	Tripped		
.642	.483	6.5	.465	8.7	36	Untripped				
⊠	^a 26	Morrisette, Stone, and Cary	0.276×10^4	0.156	8.0	0.70	13.4	<0.1	Untripped	
			.445	.269	8.0	.70	12.8	17	Untripped	
			.475	.274	8.0	.70	10.0	12	Tripped	
			.497	.281	8.0	.70	10.2	17	↓	
			.523	.292	8.0	.70	8.3	14		
			.608	.343	8.0	.70	7.6	13		
			.640	.386	8.0	.70	8.8	23		
			.648	.391	8.0	.70	8.6	25		
.670	.406	8.0	.70	8.9	23					
⊕	27	Wagner et al.	0.223×10^4	0.212	6.80	0.83	9.3	2.6		Untripped
			.318	.218	6.80	.83	9.0	6.4		↓
			.548	.220	6.80	.83	7.7	18.5		

^aValue of N obtained directly from report and not from replot of velocity profile.

TABLE I.- KEY FOR TURBULENT-BOUNDARY-LAYER DATA FOR FLAT PLATE
AND AXISYMMETRIC BODIES - Continued

(a) Compressible data - Continued

Symbol	Reference		$Re_{e,\theta}$	θ , mm	Me	T_w/T_t	N	$\frac{(\Delta x)_{tr}}{\delta}$	Transition
	Number	Author							
Flat plate									
▷	28	Higgins and Pappas	0.275×10^4	0.131	2.4	0.956	7.5	<0.1	Untripped ↓
			.230	.135	2.4	1.027	8.0	<.1	
			.220	.149	2.4	1.096	8.5	<.1	
			.210	.159	2.4	1.170	9.3	<.1	
			.182	.183	2.4	1.305	9.3	<.1	
◁	29	Korkegi	0.404×10^4	0.411	5.80	0.906	6.7	25	Tripped ↓
			.343	.405	5.8	.906	6.45	30	
			.278	.416	5.8	.906	5.8	34	
▷	30	Sterrett and Emery	0.229×10^4	0.129	4.8	0.916	9.3	6	Untripped ↓
			.269	.152	4.8	.916	9.75	17	
			.323	.183	4.8	.916	8.2	26	
			.241	.104	5.8	.909	14.0	<.1	
			.332	.143	5.8	.909	10.0	<.1	
◻	31	Moore	0.938×10^4	0.208	4.95	0.886	8.0	45	Tripped ↓
			.939	.207	4.95	.892	8.8	50	
			.445	.220	4.95	.585	6.1	41	
			.351	.229	4.95	.496	6.2	40	
◆	^a 32	Richards	0.171×10^4	0.081	8.2	0.397	9.0	2	Tripped ↓
			.218	.099	8.2	.397	9.0	8	
			.259	.117	8.2	.397	9.0	15	
◁	33	Monaghan and Cooke	0.311×10^4	0.345	2.82	1.35	7.02	30	Untripped ↓
			.194	.211	2.82	1.35	7.30	16	
			.279	.371	2.82	.94	6.88	38	
			.218	.284	2.82	.94	7.20	42	
			.149	.179	2.82	.94	6.95	42	
◁	34	Ladenburg and Bershader	0.1028×10^4	0.092	2.35	0.969	13.5	<0.1	Untripped
◻	35	Woodruff and Lorenz	0.760×10^4	0.483	6.88	0.754	6.85	31	Tripped ↓
			.612	.389	6.88	.754	6.88	32	
●	^a 36	Nothwang	1.350×10^4	0.300	3.03	0.933	6.0	41	Tripped
◊	37	Moore and Harkness	5.730×10^4	----	2.91	0.935	7.82	---	-----
Cone									
◊	38	Allen and Monta	1.515×10^4	0.680	1.61	0.945	7.42	---	Tripped ↓
			.202	.750	1.61	.945	6.72	---	
			.398	.869	1.61	.945	6.42	---	
			.110	.317	1.61	.945	6.00	---	
			.767	.339	1.61	.945	7.58	---	
			.530	.388	1.61	.945	6.45	---	
			.207	.444	1.61	.945	6.76	---	
			.793	.455	2.20	.922	7.50	77	
			.515	.476	2.20	.922	6.96	73	

^aValue of N obtained directly from report and not from replot of velocity profile.

TABLE I.- KEY FOR TURBULENT-BOUNDARY-LAYER DATA FOR FLAT PLATE
AND AXISYMMETRIC BODIES - Continued

(a) Compressible data - Continued

Symbol	Reference		Re_{θ}	θ , mm	Me	T_w/T_t	N	$\frac{(\Delta x)_{tr}}{\delta}$	Transition	
	Number	Author								
◇	38	Allen and Monta	Cone						62 95 85 91 87 74 69 64 85	Tripped ↓
			0.213×10^4	0.568	2.20	0.922	6.85			
			1.086	.617	2.20	.922	7.75			
			.707	.655	2.20	.922	7.42			
			.281	.758	2.20	.922	7.04			
			.413	.234	2.20	.922	6.32			
			.273	.253	2.20	.922	6.76			
			.563	.317	2.20	.922	8.17			
			.154	.430	2.20	.922	6.78			
			.400	.371	2.20	.922	7.06			
◡	a39	Bradfield	0.218×10^4	0.152	3.7	0.928	7.0	77	Tripped	
			.374	.133	3.7	.928	7.0	88	↓	
			.213	.150	3.7	.928	7.0	78	↓	
			.185	.131	3.7	.928	7.0	51	↓	
			.205	.145	3.7	.928	7.0	79	↓	
◑	40	Maddalon and Henderson	0.297×10^4	0.052	15.6	1.0	15.61	---	Untripped	
			.313	.052	16.6	1.0	16.20	5	↓	
◑	41	Henderson et al.	.244	.043	12.7	1.0	14.80	8	↓	
			.205	.056	7.5	1.0	16.34	27	↓	
▲	a42	Graber, Weber, and Softley	.128	.058	7.6	1.0	15.55	---	↓	
			0.363×10^4	0.432	10.3	0.214	6.0	---	Untripped	
			.232	.713	10.2	.214	5.6	28	↓	
◑	43	Martellucci, Rie, and Sontowski	.201	.648	10.4	.214	5.4	18	↓	
			0.303×10^4	0.240	6.77	0.950	14.0	11	Untripped	
◑	44	Softley and Sullivan	.325	.257	6.77	.923	12.0	26	↓	
			0.179×10^4	0.574	10.2	0.214	3.08	29	Untripped	
◡	45	Bradfield, DeCoursin, and Blumer	0.140×10^4	0.0625	3.1	0.93	9.8	61	Untripped	
			.321	.0640	3.1	.93	9.0	66	↓	
			1.092	.173	3.1	.93	8.4	72	↓	
			.193	.0455	3.1	.93	10.3	48	Tripped	
			.272	.0646	3.1	.93	8.0	62	↓	
			.401	.0958	3.1	.93	9.3	83	↓	
			.784	.174	3.1	.93	7.8	93	↓	
□	46	Adcock, Peterson, and McRee	0.218×10^4	0.067	5.95	0.900	13.00	<0.1	Tripped	
			.325	.100	5.95	.897	10.00	<1.0	↓	
			.402	.124	5.95	.900	9.00	11	↓	
			.496	.153	5.96	.917	9.00	23	↓	
			.560	.172	5.96	.897	9.00	21	↓	
			1.350	.417	6.02	.890	8.12	53	↓	
			1.395	.427	6.02	.890	9.00	56	↓	
			1.485	.457	6.02	.888	8.76	60	↓	
			1.436	.447	6.02	.897	8.94	60	↓	

^aValue of N obtained directly from report and not from replot of velocity profile.

TABLE I.- KEY FOR TURBULENT-BOUNDARY-LAYER DATA FOR FLAT PLATE
AND AXISYMMETRIC BODIES - Continued

(a) Compressible data - Continued

Symbol	Reference		Re_{θ}	θ , mm	Me	T_w/T_t	N	$\frac{(\Delta x)_{tr}}{\delta}$	Transition				
	Number	Author											
Cone													
◊	47	Stroud and Miller	0.276×10^4	0.310	6.46	0.671	5.26	47	↓ Tripped				
			.199	.483	7.51	.818	7.80	40					
			.443	.500	7.53	.856	7.15	40					
			.578	.637	7.71	.429	6.44	38					
			.378	.429	7.46	.373	8.6	45					
			.499	.315	5.95	.550	9.97	31					
			.245	.295	5.90	.576	8.35	42					
			.461	.330	5.78	.888	7.50	44					
			.250	.488	4.62	.900	5.45	37					
			1.308	.655	4.81	.674	5.74	28					
			1.006	.505	4.90	.900	6.44	38					
			⊕	48	Samuels, Peterson, and Adcock	0.360×10^4	0.103	5.92		0.454	8.8	6	↓ Tripped
						.518	.156	5.94		.454	8.9	18	
1.291	.373	5.98				.454	7.8	56					
1.287	.404	5.98				.454	8.3	64					
1.342	.404	5.97				.454	7.8	66					
.310	.110	5.99				.400	8.4	6					
.429	.160	5.98				.400	8.0	19					
1.061	.383	6.08				.400	7.5	56					
1.162	.429	6.04				.400	6.7	61					
◊	49	O'Donnell	0.660×10^4	0.178	2.41	0.933	7.15	44	↓ Untripped				
			.299	.104	2.41	.933	6.70	26					
			.536	.145	2.41	.933	7.10	36					
			.380	.132	2.41	.933	6.85	35					
			.482	.168	2.41	.933	7.20	43					
			.442	.119	2.41	.933	7.00	29					
◊	250	Brinich and Diaconis	1.095×10^4	0.424	3.08	0.926	7.65	70	↓ Tripped Untripped Untripped Tripped				
			1.094	.423	3.025	.924	7.00	63					
			.650	.394	3.06	.930	6.56	61					
			.450	.686	2.98	.924	6.35	56					
◊	51	Hoydysh and Zakkay	3.800×10^4	0.325	5.75	0.634	7.23	73	Untripped				
Ogive cylinder													
◊	52	Aircraft Div., Douglas Air- craft Co., Inc.	7.024×10^4	0.223	0.85	0.935	7.8	89	↓ Tripped				
			3.54	.648	1.98	.898	7.1	101					
			3.442	1.250	2.98	.937	8.3	112					
			1.316	.477	2.98	.954	7.0	101					
			5.76	1.044	2.98	.920	9.5	115					
			11.79	1.425	2.98	.920	8.8	105					
			4.05	1.029	4.88	.764	8.0	99					
			4.615	.838	4.88	.764	7.65	114					

^aValue of N obtained directly from report and not from replot of velocity profile.

TABLE I.- KEY FOR TURBULENT-BOUNDARY-LAYER DATA FOR FLAT PLATE
AND AXISYMMETRIC BODIES - Continued

(a) Compressible data - Concluded

Symbol	Reference		Re_{θ}	θ , mm	M_e	T_w/T_t	N	$\frac{(\Delta x)_{tr}}{\delta}$	Transition
	Number	Author							
			Body of revolution (NACA RM-10)						
◁	53	Swanson, Buglia, and Chauvin	7.78×10^4	2.423	1.43	0.76	8.5	90	Untripped ↓
			7.81	2.210	1.64	.72	9.3	89	
			6.71	2.367	1.43	.83	8.5	88	
			5.58	2.603	1.23	.95	7.0	84	
			5.52	2.616	1.43	.95	8.0	76	
			7.27	2.174	2.58	.59	9.4	82	
			9.19	2.372	3.32	.46	9.3	57	
			8.32	2.128	3.67	.41	8.0	57	
			7.88	2.174	3.53	.49	7.9	82	
			6.07	2.050	3.31	.49	8.0	82	
			3.57	1.829	2.89	.80	7.2	86	
			2.40	1.844	2.57	.81	7.7	75	
			1.35	1.648	2.82	1.02	6.1	57	
			.897	1.900	2.05	1.17	5.9	---	
			Pipe extension of nozzle						
◁	54	Jones and Feller	5.96×10^4	1.626	5.82	0.66	8.4	66	Untripped ↓
			3.31	1.727	5.95	.66	8.3	52	
			1.54	1.905	5.83	.66	7.1	50	
			1.03	2.083	5.76	.66	7.1	47	
			7.71	2.083	5.79	.66	8.8	69	
			4.70	2.337	5.75	.66	8.4	63	
			2.02	2.362	5.67	.66	7.3	59	
			1.37	2.743	5.58	.66	6.7	51	
			7.97	2.337	5.69	.66	8.8	75	
			5.66	2.565	5.66	.66	8.4	73	
			Shock-tube wall						
●	55	Gooderum	0.415×10^4	1.346	1.77	0.136	4.03	61	Untripped ↓
			.477	1.547	1.77	.136	3.96	96	
			.572	1.854	1.77	.136	4.12	178	
			.618	2.007	1.77	.136	4.81	227	
▲	56	Martin	0.742×10^4	0.646	0.67	0.650	5.9	98	Untripped ↓
			1.770	1.326	1.28	.343	4.4	82	
			Cone cylinder						
◐	57	Chapman and Kester	1.374×10^4	0.528	1.98	0.954	6.44	27	Tripped

TABLE I.- KEY FOR TURBULENT-BOUNDARY-LAYER DATA FOR FLAT PLATE
AND AXISYMMETRIC BODIES - Concluded

(b) Incompressible data

Symbol	Reference		Re_{θ}	θ , mm	N	$\frac{(\Delta x)_{tr}}{\delta}$	Transition
	Number	Author					
△	58	Schubauer and Klebanoff	0.231×10^4	1.3868	4.2	<0.1	Untripped
			.287	1.435	5.5	<.1	↓
			.280	1.676	5.0	<.1	↓
◀	59	Patel and Head	0.210×10^4	2.11	5.3	---	Untripped
			.580	5.37	5.8	---	↓
▶	60	Wooldridge and Willmarth	3.800×10^4	8.001	8.5	---	Untripped
			4.300	8.001	8.2	---	↓
▽	61	Favre, Gaviglio, and Dumas	0.164×10^4	1.999	4.5	---	Tripped
			.189	2.299	4.4	---	↓
			.263	3.200	5.1	---	↓
			.308	3.746	5.1	---	↓
			.357	4.343	5.4	---	↓
▽	^a 62	Ross	Eight investigations of incompressible velocity profiles				
⊕	63	van der Hegge Zijnen	0.151×10^4	1.788	5.1	---	-----
			.189	1.700	4.7	---	-----
			.147	.920	4.9	---	-----
			.169	1.064	4.9	---	-----
			.207	1.284	4.7	---	-----
			.262	1.614	5.1	---	-----
			.284	1.690	4.9	---	-----

^aValue of N obtained directly from report and not from replot of velocity profile.

TABLE II.- KEY FOR TURBULENT-BOUNDARY-LAYER DATA
FOR TWO-DIMENSIONAL NOZZLE WALLS

Symbol	Reference		$Re_{e,\theta}$	θ , mm	M_e	T_w/T_t	N
	Number	Author					
◁	34	Ladenburg and Bershader	4.904×10^4	1.466	2.35	0.969	6.7
◇	37	Moore and Harkness	70.2×10^4	8.118	2.67	0.940	10.3
◊	^a 64	Bertram and Neal	3.00×10^4	2.388	6.80	0.50	6.3
			1.30	3.048	6.80	.50	5.0
□	^a 64	Bertram and Neal	4.90×10^4	1.854	6.00	0.63	9.0
			2.40	1.778	6.00	.63	7.8
			1.90	1.981	6.00	.63	7.4
○	65	Lobb, Winkler, and Persh	0.535×10^4	0.624	4.93	0.924	5.89
			.648	.708	5.01	.712	6.82
			.795	.815	5.03	.576	6.54
			.737	.871	5.06	.532	6.66
			1.160	.643	5.75	.813	6.19
			1.124	.745	5.79	.694	6.39
			1.140	.865	5.82	.567	6.14
			.855	.784	6.83	.614	5.86
			.840	.825	6.78	.514	5.65
			1.260	.903	6.83	.507	5.63
			.796	.882	6.78	.455	5.61
			.813	1.052	7.67	.465	5.13
			.954	1.140	8.18	.459	5.46
△	66	Spivack	1.339×10^4	0.366	2.81	0.937	6.64
			1.230	.366	2.77	.939	6.29
			1.203	.363	2.77	.940	6.78
			1.169	.330	2.83	.939	6.88
◓	67	Bartle and Leadon	0.985×10^4	0.818	2.00	0.954	5.40
			1.050	.847	2.00	.954	5.90
			1.050	.902	2.00	.954	6.21
			1.100	.914	2.00	.954	6.20
			1.170	1.369	3.20	.930	5.47
			1.230	1.438	3.20	.930	5.54
			1.420	1.656	3.20	.930	5.97
			1.580	1.841	3.20	.930	5.87

^aValue of N obtained directly from report and not from replot of velocity profile.

TABLE II.- KEY FOR TURBULENT-BOUNDARY-LAYER DATA
FOR TWO-DIMENSIONAL NOZZLE WALLS - Continued

Symbol	Reference		$Re_{e,\theta}$	θ , mm	Me	T_w/T_t	N
	Number	Author					
⊕	68	Jeromin	1.560×10^4	0.336	3.59	0.983	5.75
			1.720	.347	2.55	.960	6.02
◐	a69	Bell	0.225×10^4	1.143	4.00	0.922	14.0
			.560	1.778	4.00	.922	7.1
			.192	1.041	5.00	.912	7.1
			.280	1.016	5.00	.912	10.0
			.660	1.676	5.00	.912	6.7
◑	70	Matting et al.	0.362×10^4	0.107	7.67	1.0	9.8
			3.740	.330	4.20	1.0	9.04
			2.040	.356	4.20	1.0	7.68
			2.195	.432	2.95	1.0	8.38
◒	71	Kistler	4.0×10^4	1.422	1.72	0.961	7.00
			2.88	1.384	4.67	.916	5.33
			3.3	1.384	3.56	.926	5.86
◓	a72	Lee, Yanta, and Leonas	0.51×10^4	----	4.7	0.68	5.7
			.48	----	4.7	.68	6.7
			.59	----	4.7	.68	6.2
			.90	----	4.7	.68	6.6
			1.85	----	4.7	.68	7.35
			2.4	----	4.7	.68	7.90
			2.8	----	4.7	.68	7.2
			3.7	----	4.7	.68	8.0
			3.8	----	4.7	.68	7.0
			5.2	----	4.7	.68	8.6
			5.8	----	4.7	.68	8.2
			1.9	----	4.7	.5	6.8
			1.9	----	4.7	.5	7.8
			1.5	----	4.7	.44	6.7
1.7	----	4.7	.44	6.5			
◔	73	Kepler and O'Brien	2.1×10^4	0.889	6.00	0.800	5.0
			.77	.635	3.00	.800	6.0
◕	a74	Baron	2.700×10^4	1.600	1.47	0.964	6.9
			1.835	1.216	1.98	.947	8.1
			1.815	1.201	2.02	.947	8.7
			2.060	1.587	2.43	.935	7.8
			2.025	1.615	2.98	.923	8.2

^aValue of N obtained directly from report and not from replot of velocity profile.

TABLE II.- KEY FOR TURBULENT-BOUNDARY-LAYER DATA
FOR TWO-DIMENSIONAL NOZZLE WALLS - Continued

Symbol	Reference		Re, θ	$\theta, \text{ mm}$	Me	T_w/T_t	N
	Number	Author					
◩	75	Jackson, Czarnecki, and Monta	0.958×10^4	4.359	2.20	0.949	6.00
			1.39	3.785	2.20	.949	6.65
			5.96	2.870	2.20	.949	9.25
			7.46	4.206	2.20	.949	8.60
			2.13	5.794	2.20	.949	6.60
			12.37	4.674	1.61	.946	8.85
			9.30	3.505	1.61	.946	9.60
◪	^a 76	Brinich	0.913×10^4	0.635	1.84	0.954	9.2
			1.024	.724	1.92	.946	8.75
			1.150	.838	2.00	.946	9.2
			1.290	.940	2.00	.946	8.5
			1.496	1.092	2.00	.946	7.5
			.607	.444	2.00	.950	7.4
			.794	.597	2.05	.998	7.2
			1.085	.813	2.04	.946	7.1
			1.275	.952	2.03	.946	6.6
			1.495	1.092	2.00	.946	6.6
			1.705	1.245	2.00	.946	6.8
			2.181	1.575	1.96	.946	6.6
			◴	77	Speaker and Ailman	1.616×10^4	1.283
1.566	.947	.59				.993	8.00
1.674	.818	.90				.985	8.8
1.810	.767	1.40				.970	6.7
2.300	.912	1.81				.958	6.45
5.920	.879	2.50				.942	8.4
3.072	1.001	2.52				.942	7.0
5.320	1.252	3.45				.927	6.1
◳	78	Aeromechanics Section of Defense Research Laboratory	0.455×10^4	0.136	2.00	0.954	7.1
			.268	.156	5.00	.913	8.2
◲	79	Winter, Smith and Gaudet	8.50×10^4	6.756	2.20	0.949	9.2
			7.54	7.087	2.20	.949	8.6
			6.40	7.010	2.20	.949	8.9
◱	80	Ruptash	0.467×10^4	0.553	2.94	0.934	8.4
			.464	.546	2.87	.936	7.5
			.434	.492	2.84	.936	7.0
			.420	.463	2.77	.937	6.5

^aValue of N obtained directly from report and not from replot of velocity profile.

TABLE II.- KEY FOR TURBULENT-BOUNDARY-LAYER DATA
FOR TWO-DIMENSIONAL NOZZLE WALLS - Continued

Symbol	Reference		$Re_{e,\theta}$	θ , mm	Me	T_w/T_t	N
	Number	Author					
◻	81	Thomann	1.220×10^4	0.922	1.81	0.959	5.85
			1.100	.909	2.02	.954	6.35
△	a82	Jones	6.08×10^4	3.988	3.0	0.933	8.4
			5.34	4.064	3.0	.933	8.3
			4.62	4.115	3.0	.933	8.2
			3.15	4.369	3.0	.933	7.7
			2.25	4.826	3.0	.933	7.2
			7.13	3.505	5.0	.913	7.6
			6.40	3.607	5.0	.913	7.5
			5.50	3.683	5.0	.913	7.2
			7.37	3.404	4.5	.916	7.1
			6.60	3.759	4.5	.916	7.0
			7.00	3.810	4.0	.920	7.7
			5.33	3.962	4.0	.920	7.3
			6.82	3.886	3.5	.926	8.6
			5.69	3.988	3.5	.926	8.4
			3.33	3.759	5.5	.910	6.5
			2.91	3.861	5.5	.910	6.2
			2.11	4.013	5.5	.910	5.9
			4.71	3.886	2.5	.942	9.0
			4.37	4.013	2.5	.942	8.8
			4.75	3.810	5.0	.913	7.1
			3.88	3.937	5.0	.913	6.8
			2.95	4.089	5.0	.913	6.6
			1.77	4.216	5.0	.913	6.5
			7.50	3.683	2.0	.954	8.8
			5.18	3.835	2.0	.954	8.8
			3.07	4.166	2.0	.954	8.2
			2.13	4.318	2.0	.954	7.8
6.23	4.267	1.5	.968	8.3			
5.08	4.369	1.5	.968	8.2			
2.73	4.623	1.5	.968	7.6			
2.44	4.369	4.5	.916	6.0			
1.77	4.826	4.0	.920	6.3			
1.86	5.207	3.5	.926	7.1			

^aValue of N obtained directly from report and not from replot of velocity profile.

TABLE II.- KEY FOR TURBULENT-BOUNDARY-LAYER DATA
FOR TWO-DIMENSIONAL NOZZLE WALLS - Concluded

Symbol	Reference		$Re_{e,\theta}$	θ , mm	M_e	T_w/T_t	N			
	Number	Author								
△	a82	Jones	1.76×10^4	4.826	2.5	0.926	7.4			
			7.76	3.454	5.0	.942	9.5			
			8.45	3.556	4.5	.916	10.4			
			1.85	4.369	4.5	.916	8.2			
			7.46	3.785	4.0	.920	11.9			
			1.77	4.801	4.0	.920	8.5			
			6.90	3.505	3.5	.926	10.0			
			3.00	4.572	3.5	.926	8.1			
			7.98	3.861	3.0	.933	9.1			
			3.15	4.572	3.0	.933	8.2			
			6.98	3.785	2.5	.942	7.8			
			5.86	4.064	2.0	.954	7.9			
			3.60	4.572	1.5	.968	6.4			
			◇	83	Dershin et al.	3.184×10^4	1.405	3.20	0.93	5.0
						84	Meier	1.300×10^4	0.766	3.0
.650	.934	1.5	.97	6.8						
⊠	84	Meier	1.300×10^4	0.766	3.0	0.93	7.1			
			.650	.934	1.5	.97	6.8			
△	b85	Thomke and Roshko	8.65×10^4	5.194	2.99	1.10	10.4			
			11.10	5.016	2.98	1.10	10.8			
			16.62	5.187	2.98	.92	10.5			
			27.31	4.686	2.98	.95	10.8			
			10.27	5.283	2.49	1.10	10.2			
			19.67	4.481	2.48	1.10	10.4			
			14.06	5.024	1.99	1.15	9.2			
			22.19	4.988	4.40	.89	10.1			
			13.84	5.060	4.40	.95	10.3			
			10.16	5.237	4.92	.90	9.5			
			20.53	5.387	3.94	.87	9.9			
			32.34	4.849	3.94	.93	10.7			
			9.37	5.253	3.48	1.00	10.1			
			14.42	5.024	3.48	1.00	11.0			
			22.73	5.296	3.45	.95	10.8			
			19.69	6.124	2.96	.93	10.7			
			35.20	5.969	2.95	.95	10.9			
			25.58	5.730	2.46	1.1	10.0			
			18.60	6.589	1.95	1.1	8.7			
			26.63	5.878	4.40	.89	10.1			
23.96	6.198	3.93	.87	10.4						
38.39	5.700	3.93	.93	10.8						
27.54	6.388	3.43	.94	10.2						

^aValue of N obtained directly from report and not from replot of velocity profile.

^bData were measured on test-section floor at stations 84.0 inches (2.13 m) and 172.2 inches (4.37 m) and were used to calculate the boundary-layer properties listed in table I of reference 85.

TABLE III.- KEY FOR TURBULENT-BOUNDARY-LAYER DATA FOR
AXISYMMETRIC NOZZLE WALLS

Symbol	Reference		Re_{θ}	θ , mm	Me	T_w/T_t	N	Gas	Nozzle configuration
	Number	Author							
○	a9	Scaggs	0.279×10^4	4.801	6.65	0.312	3.31	Air ↓	Contoured ↓
			.377	4.712	11.30	.275	3.69		
			.206	3.353	6.46	.317	4.34		
			.628	3.444	6.72	.408	4.85		
			.258	3.353	11.52	.268	4.92		
			.447	2.454	11.40	.301	6.16		
◡	10	Clark and Harvey	0.294×10^4	1.711	19.41	0.17	5.7	Nitrogen ↓	Contoured ↓
			.397	1.846	19.47	.17	5.6		
◤	54	Jones and Feller	4.57×10^4	1.321	5.98	0.66	9.3	Air ↓	Contoured ↓
			2.58	1.346	5.95	.66	8.8		
			1.34	1.651	5.87	.66	7.8		
			.81	1.753	5.87	.66	7.65		
◇	86	Hill	0.229×10^4	0.305	9.10	0.495	4.23	Nitrogen ↓	Conical ↓
			.228	.314	9.07	.476	4.36		
			.145	.240	10.04	.443	3.99		
			.170	.225	10.06	.426	4.36		
			.250	.300	8.27	.421	4.03		
◡	87	Michel	0.973×10^4	0.793	9.6	0.273	8.4	Air ↓	Conical ↓
			1.125	1.105	10.55	.273	6.00		
			.922	1.141	10.95	.273	5.54		
◊	88	Burke	1.200×10^4	2.68	8.25	0.153	4.1	Air ↓	Conical ↓
			.184	3.33	16.3	.118	4.16		
			.240	4.45	14.0	.118	4.09		
			.317	4.68	12.61	.117	2.71		
			.353	5.80	10.76	.123	3.09		
			.288	7.32	8.86	.122	2.51		
◊	89	Shall	0.094×10^4	0.874	11.85	0.312	6.0	Air ↓	Contoured ↓
			.163	.800	12.07	.344	6.57		
◊	90	Tulin and Wright	2.90×10^4	4.60	0.5	0.94	7.8	Air ↓	Contoured ↓
			3.34	4.44	.69	.94	7.9		
			2.87	3.56	.88	.94	8.0		
			2.79	3.73	.97	.94	9.4		
			3.32	4.01	1.19	.94	9.3		

^aValue of N obtained directly from report and not from replot of velocity profile.

TABLE III.- KEY FOR TURBULENT-BOUNDARY-LAYER DATA FOR
 AXISYMMETRIC NOZZLE WALLS - Concluded

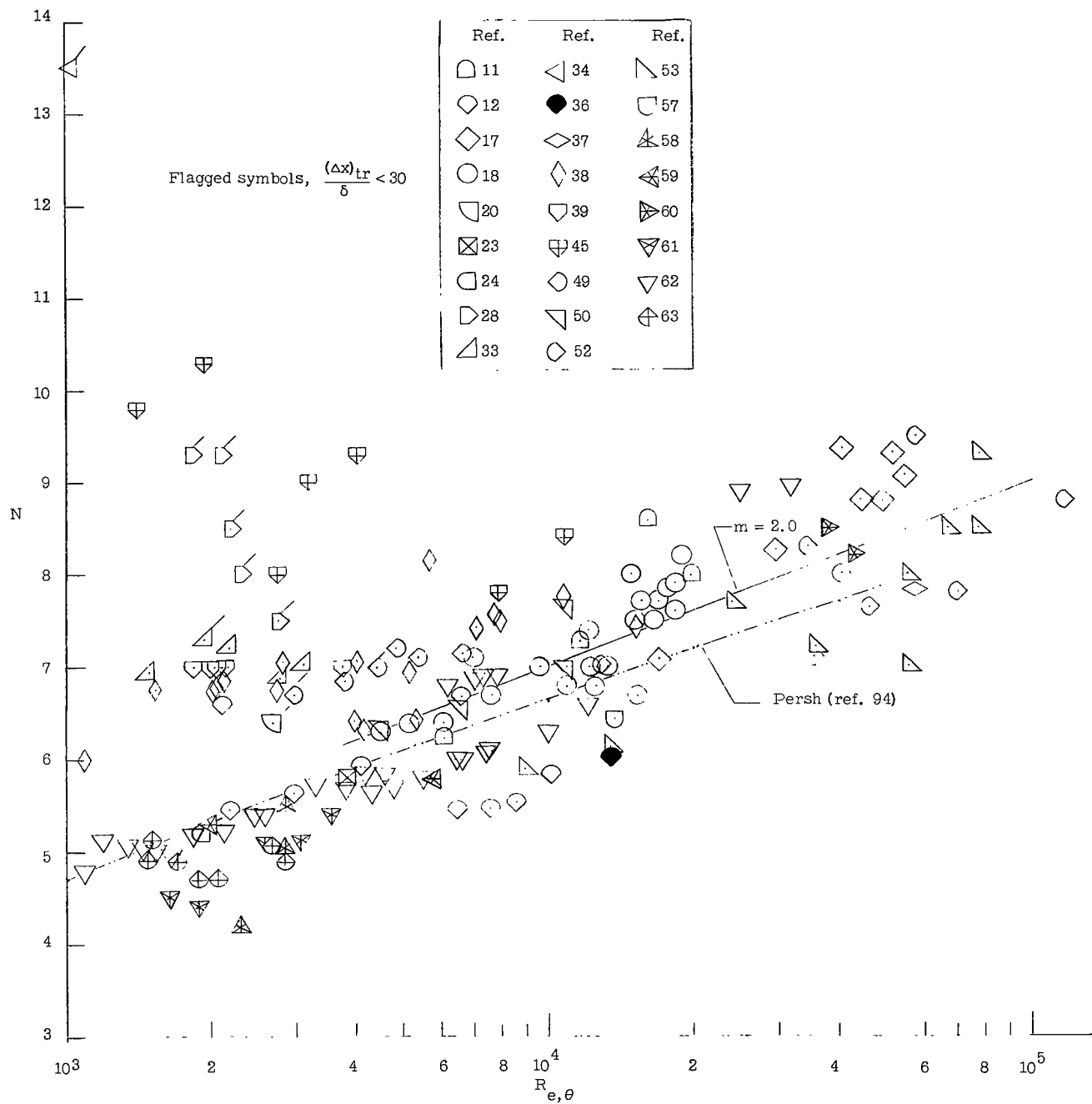
Symbol	Reference	Re_{θ}	θ , mm	M_e	T_w/T_t	N	Gas	Nozzle configuration	
	Number	Author							
◐	91	Perry and East	1.67×10^4	0.917	8.87	0.350	5.7	Air ↓	Conical ↓
			3.13	.861	9.05	.317	5.4		
			.663	.759	11.27	.319	6.3		
			1.384	1.05	11.60	.259	6.1		
▽	a92	Matthews and Trimmer	1.725×10^4	5.055	5.93	0.66	7.0	Air ↓	Contoured ↓
			3.179	4.750	5.91	.65	9.8		
			5.245	4.089	5.95	.64	10.3		
			1.247	8.636	7.90	.39	6.5		
			2.244	7.950	7.95	.39	8.5		
			4.196	7.391	7.96	.39	9.5		
			5.942	6.731	8.02	.40	9.8		
			7.394	6.553	8.04	.40	10.4		
			1.385	12.751	9.86	.32	6.0		
			2.245	11.405	10.01	.31	6.8		
			2.256	8.280	10.06	.30	7.2		
			3.192	8.534	10.10	.29	8.4		
			4.695	7.950	10.10	.28	10.0		
5.736	8.611	10.18	.27	10.0					
△	93	Banner and Williams	0.209×10^4	0.874	7.0	0.512	6.3	Air	Conical
◻		Feller (Unpublished)	1.007×10^4	4.981	7.84	0.430	6.44	Air ↓	Contoured ↓
			1.626	4.333	7.90	.416	7.34		
			2.239	3.246	7.96	.410	8.44		
			3.125	2.400	7.99	.435	8.48		
△		Watson (Unpublished)	1.140×10^4	1.067	20.30	1.000	13.25	Helium	Contoured
⊗		Blackstock ^b (Unpublished)	3.130×10^4	6.495	10.33	0.326	5.26	Air ↓	Contoured (square cross section)
			2.044	7.148	10.33	.328	4.86		
			1.295	8.705	10.33	.333	4.90		

^aValue of N obtained directly from report and not from replot of velocity profile.

^bPreliminary data, no calibration of T_t probe.

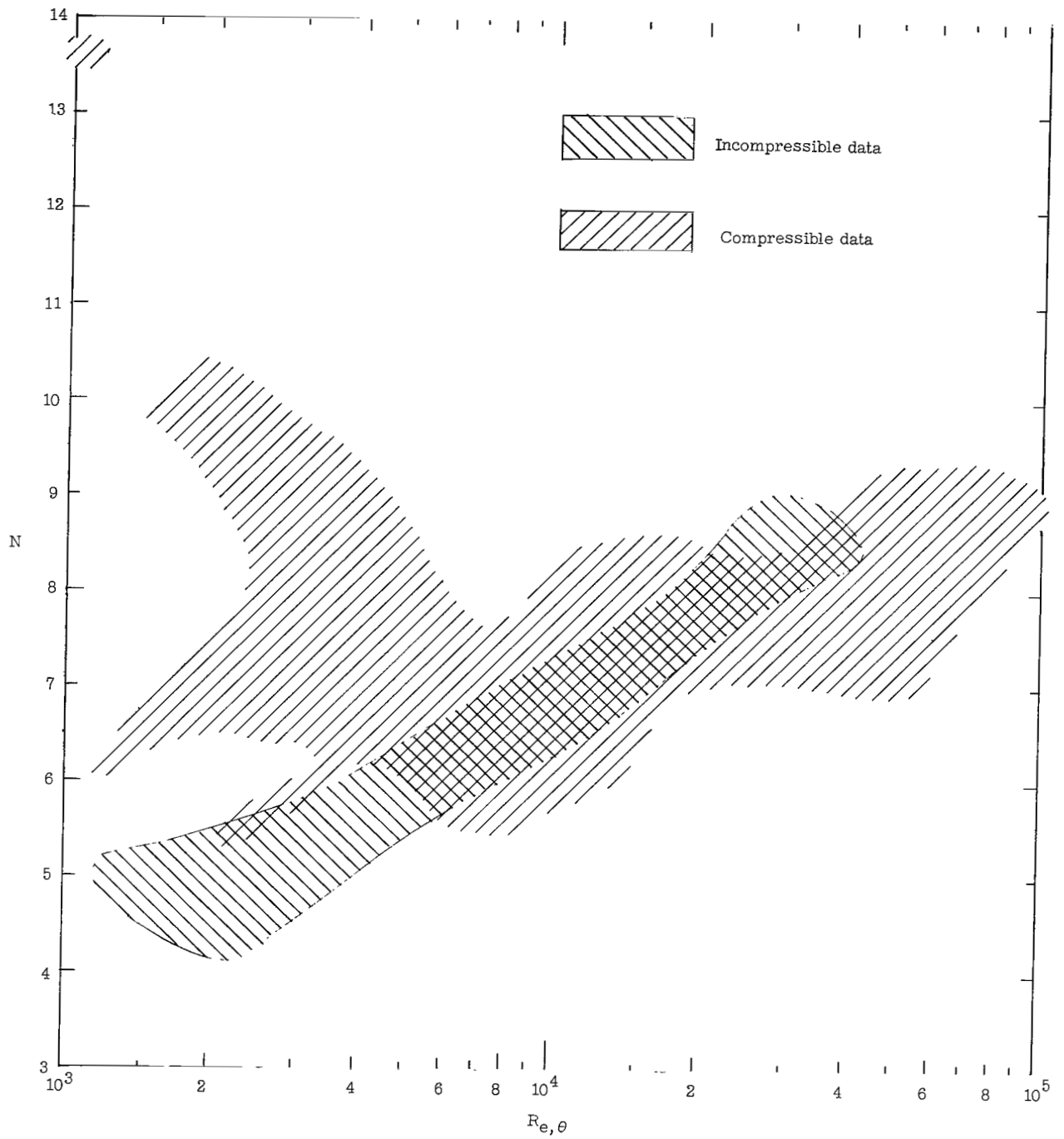
TABLE IV.- VALUES OF N AS FUNCTIONS OF $R_{e,\theta}$
 $[N = m \log_{10} R_{e,\theta} + b]$

M_e	T_w/T_t	m	b	$R_{e,\theta}$	Figure
Flat-plate class					
<4.0	1.35 to 0.66	2.0	-1.00	4×10^3 to 10^5	1(a)
>4.0	1.0 to 0.66	2.0	-.5	3.2×10^3 to 4.5×10^4	1(c)
>.67	0.66 to 0.35	2.0	-1.0	3.5×10^3 to 10^5	2
Two-dimensional nozzle wall					
>0.42	1.0 to 0.66	5.0	-15.2	1.8×10^4 to 1.4×10^5	5
>4.7	0.66 to 0.35	5.0	-14.2	8×10^3 to 5×10^4	6
Axisymmetric nozzle wall					
>0.5	0.66 to 0.35	5.0	-13.5	3.3×10^3 to 8.0×10^4	7
>6.5	0.1 to 0.35	5.0	-14.0	3.0×10^3 to 6×10^4	8



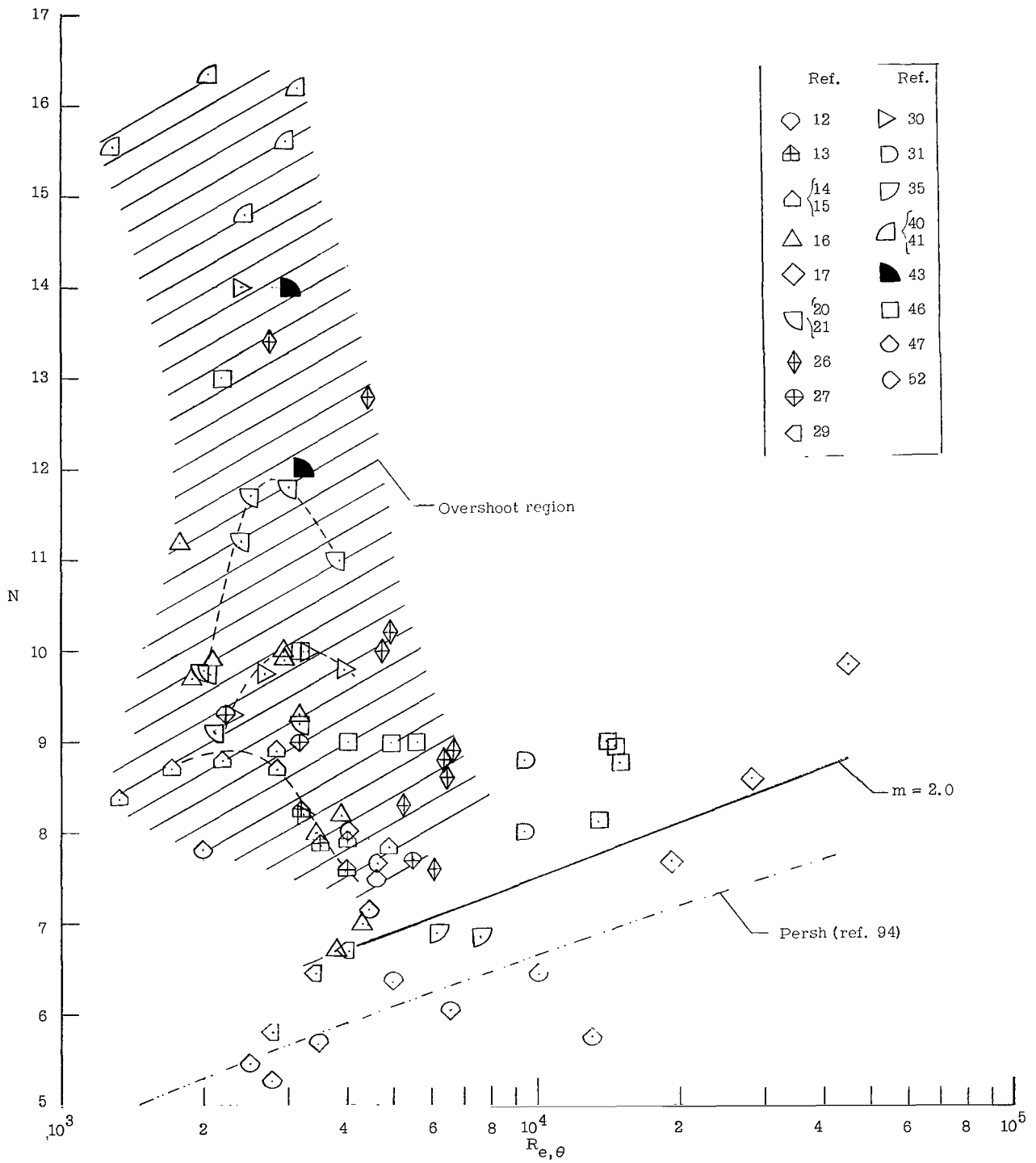
(a) $M_e < 4.0$; $0.66 < T_w/T_t \leq 1.35$.

Figure 1.- Variation of N with Re_θ for flat plates, cones, and axisymmetric bodies. Key to symbols is presented in table I.



(b) Comparison of incompressible and compressible data. $M_e < 4.0$; $0.66 < T_w/T_t \leq 1.0$.

Figure 1.- Continued.



(c) $M_e > 4.0$; $0.66 < T_w/T_t \leq 1.0$.

Figure 1.- Concluded.

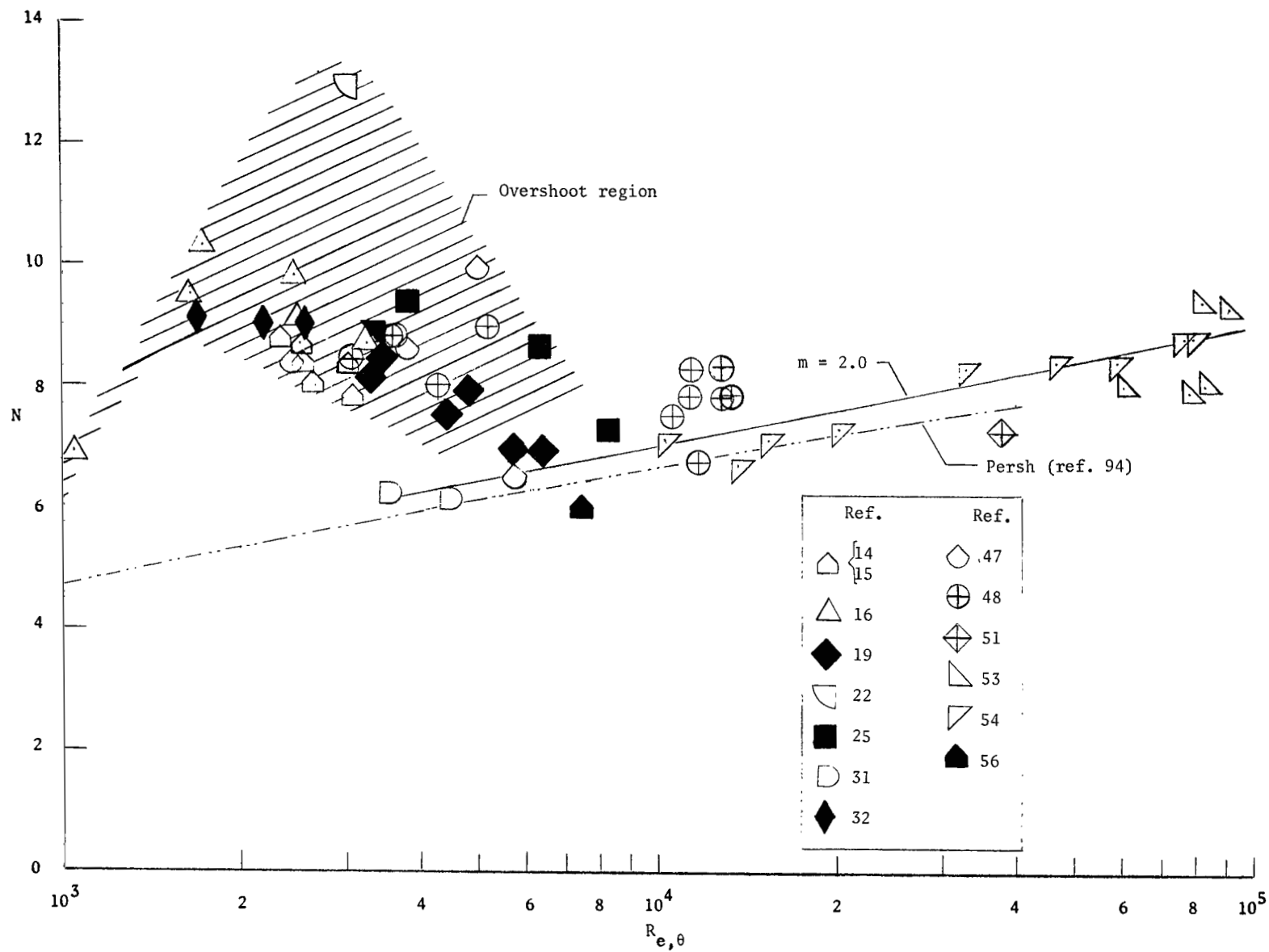


Figure 2.- Variation of N with Re_{θ} for flat plates, cones, and hollow cylinders for $0.35 < T_w/T_t \leq 0.66$. Key to symbols is presented in table I.

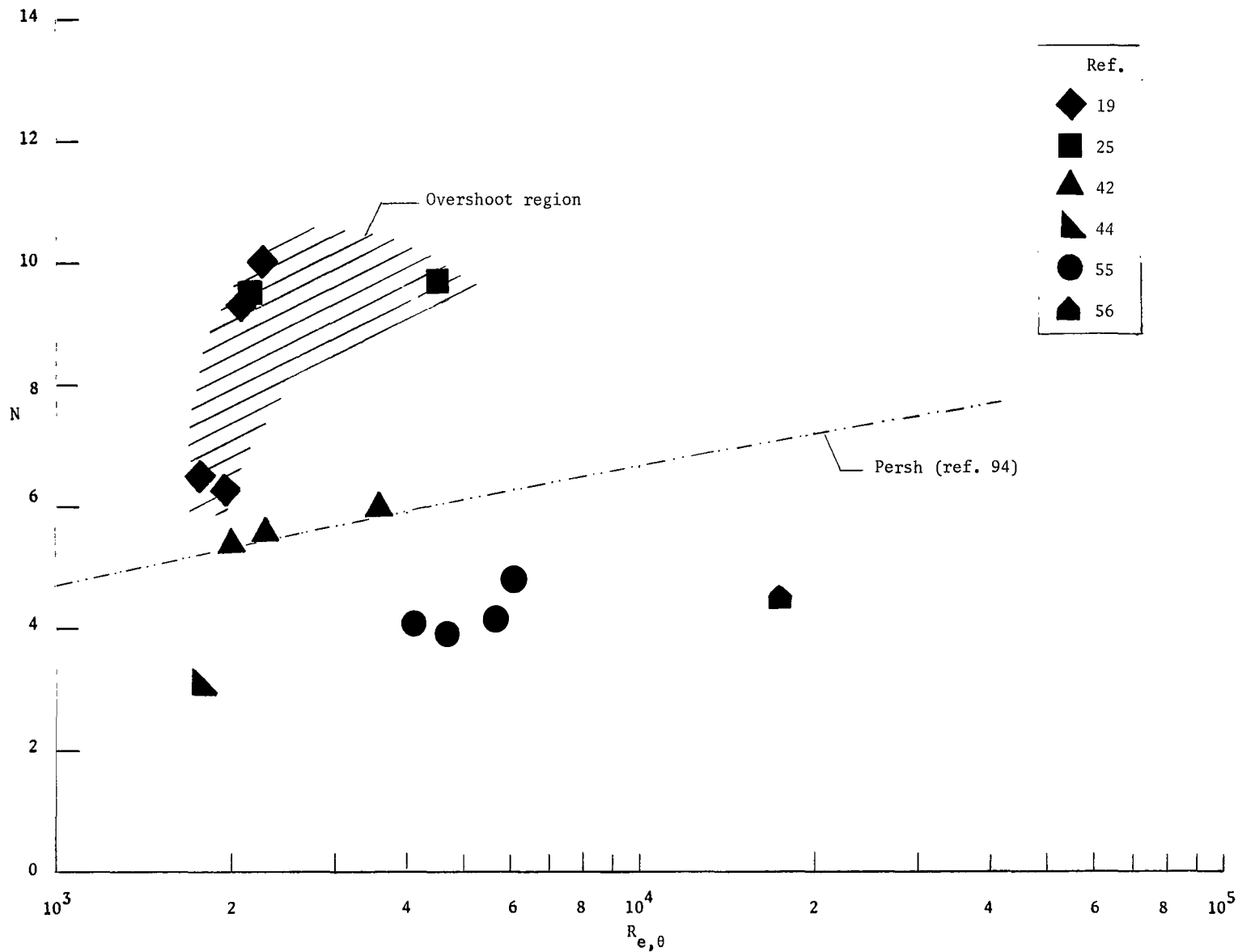
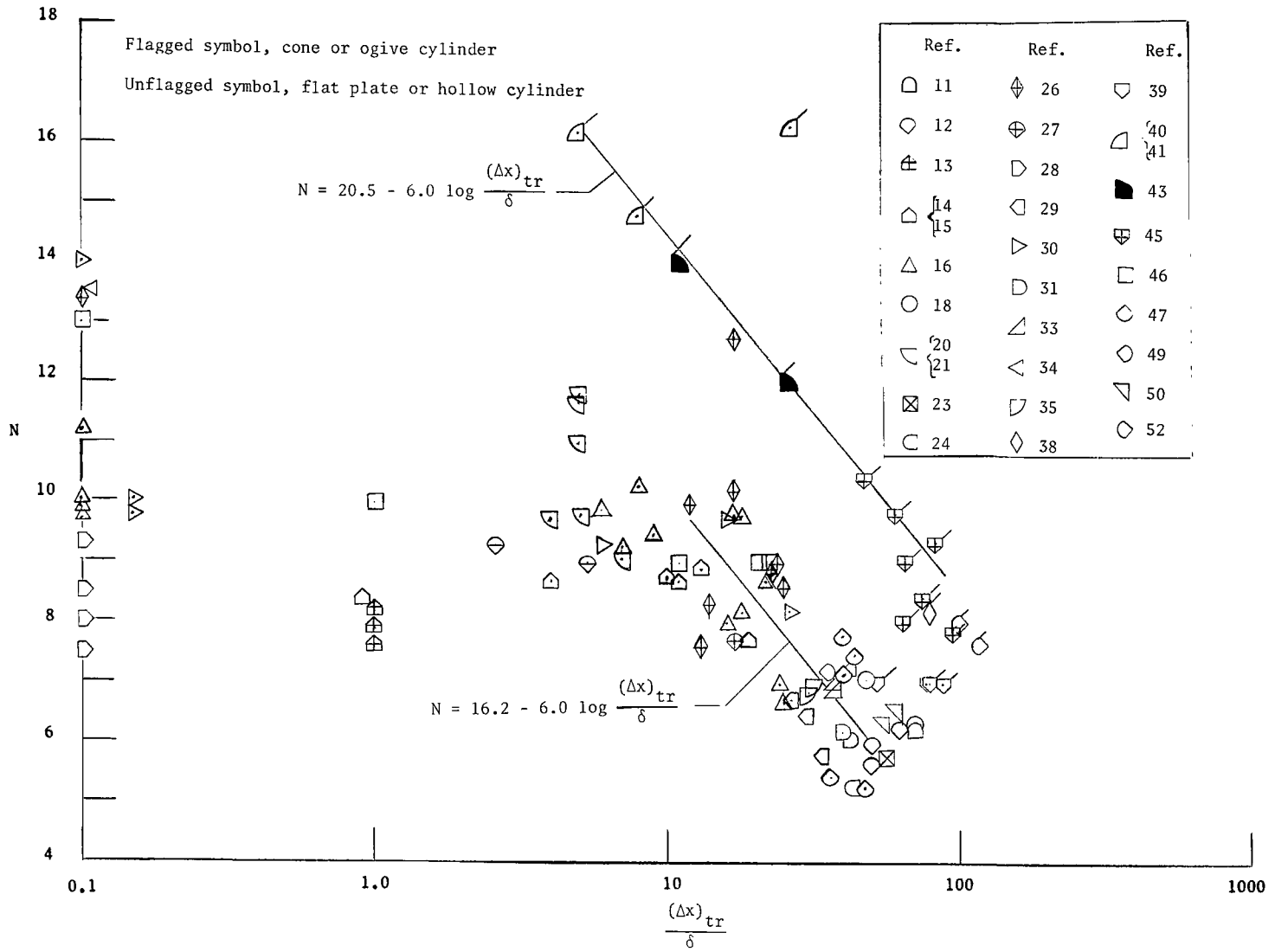
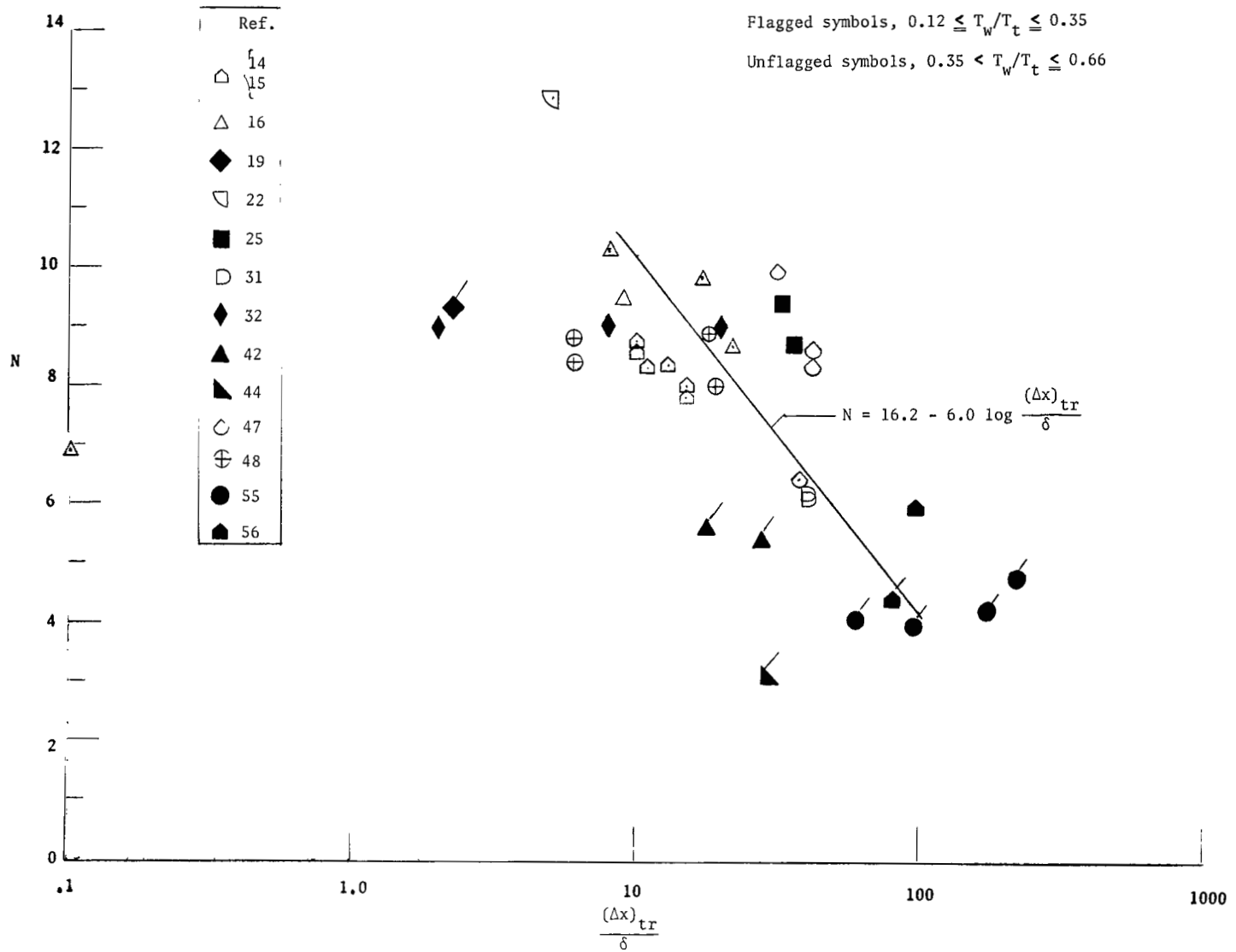


Figure 3.- Variation of N with $Re_{e,\theta}$ for flat plates, cones, and hollow cylinders for $0.12 \leq T_w/T_t \leq 0.35$. Key to symbols is presented in table I.



(a) $0.66 < T_w/T_t \leq 1.0$.

Figure 4.- Variation of N with number of boundary-layer thicknesses from beginning of turbulent flow for $Re_{e,\theta} < 8000$. Key to symbols is presented in table I.



(b) $0.12 \leq T_w/T_t \leq 0.66$.

Figure 4.- Concluded.

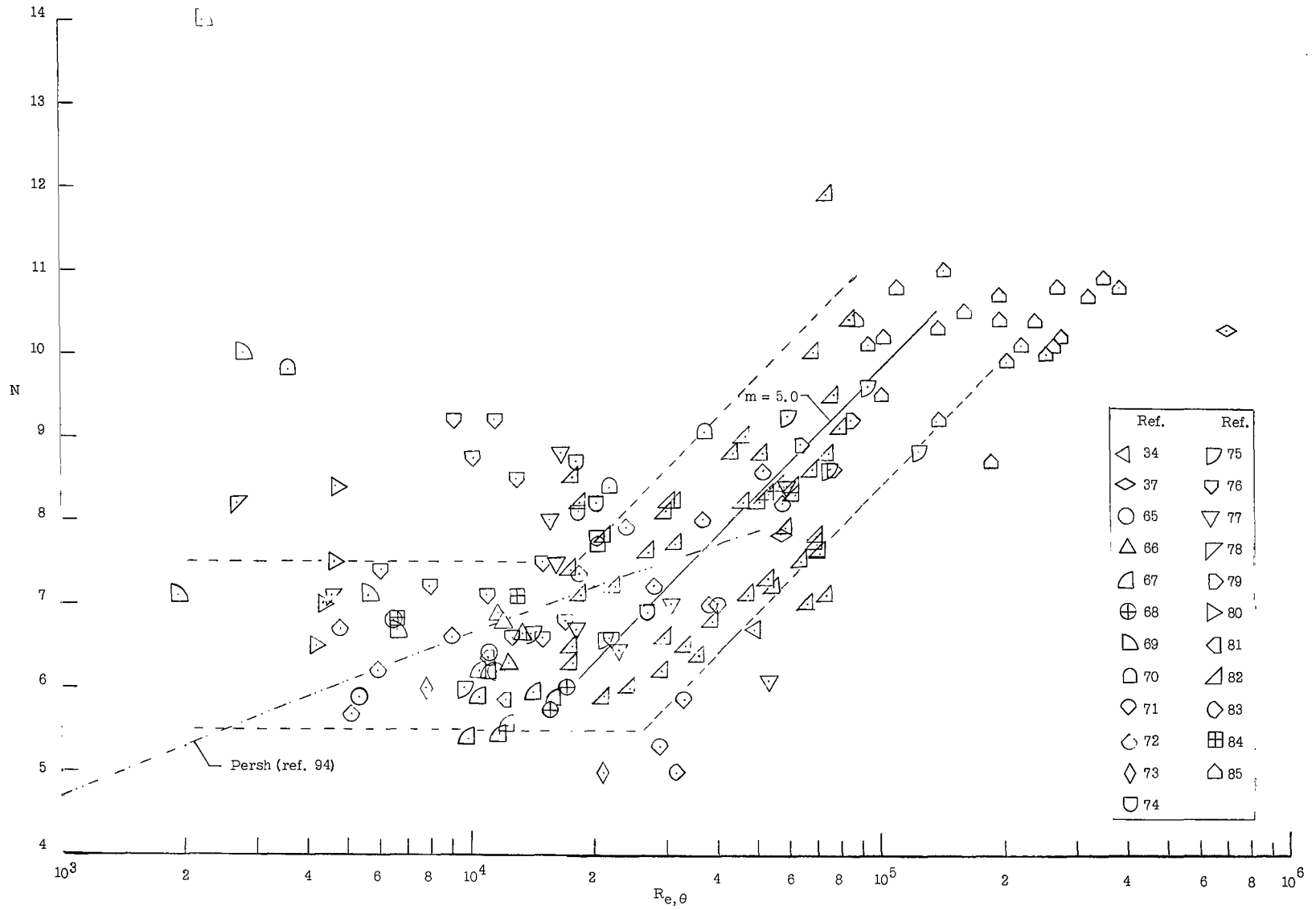


Figure 5.- Variation of N with $Re_{e,\theta}$ for two-dimensional nozzle walls at $0.66 < T_w/T_t \leq 1.0$. Key to symbols is presented in table II.

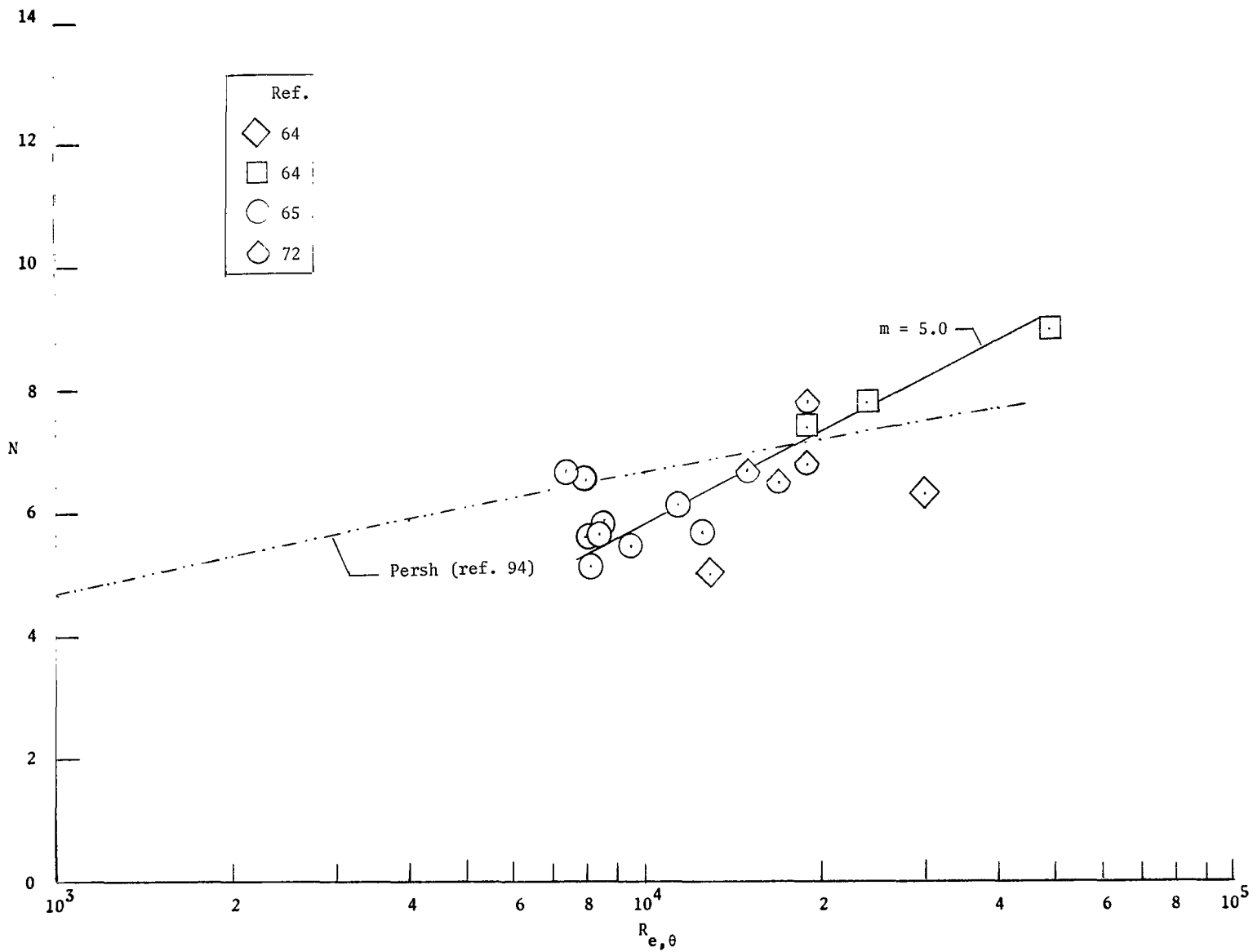


Figure 6.- Variation of N with Re, θ for two-dimensional nozzle walls at $0.35 < T_w/T_t \leq 0.66$. Key to symbols is presented in table II.

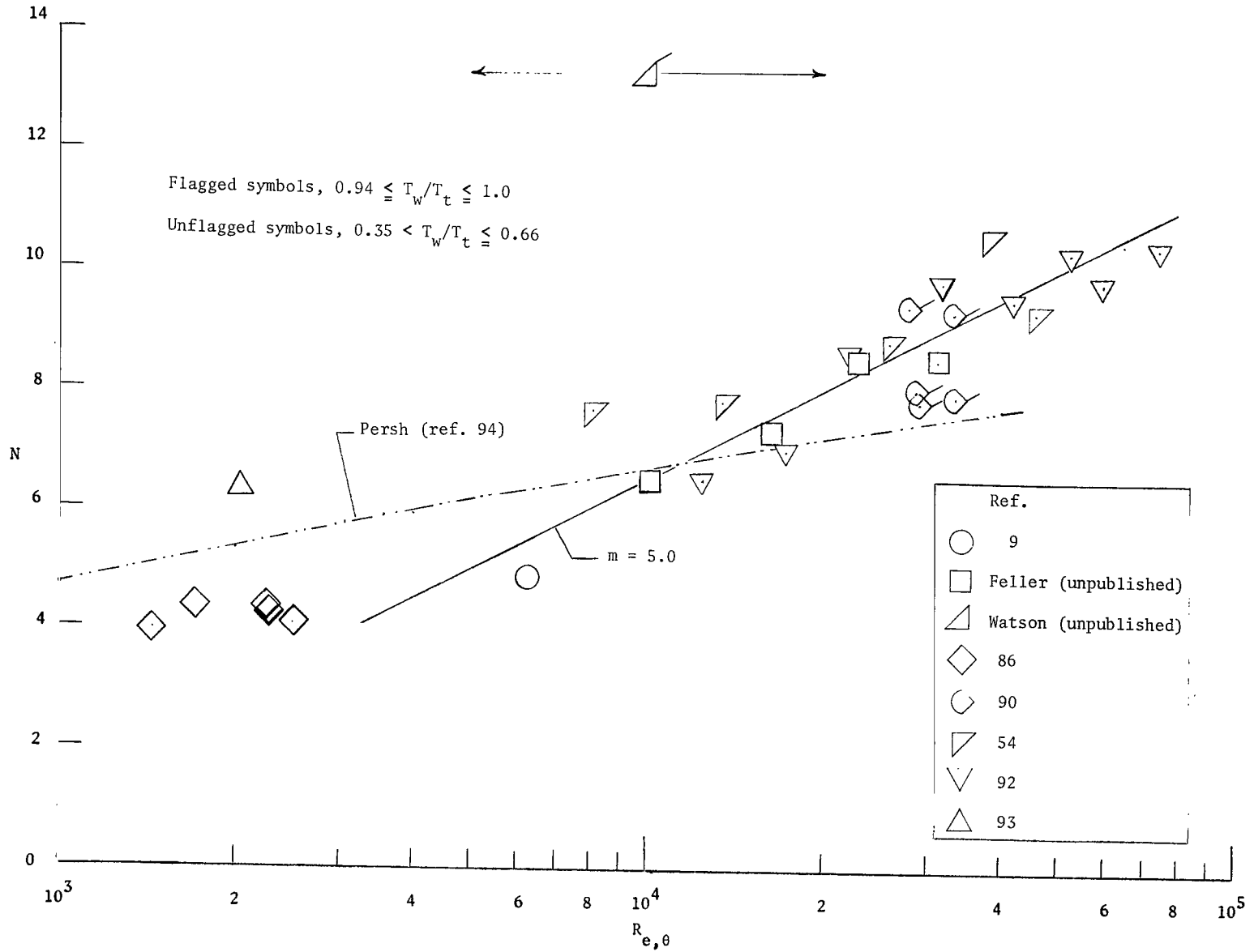


Figure 7.- Variation of N with Re_{θ} for axisymmetric nozzle walls at near-adiabatic and moderately cool wall-to-total temperature ratios. Key to symbols is presented in table III.

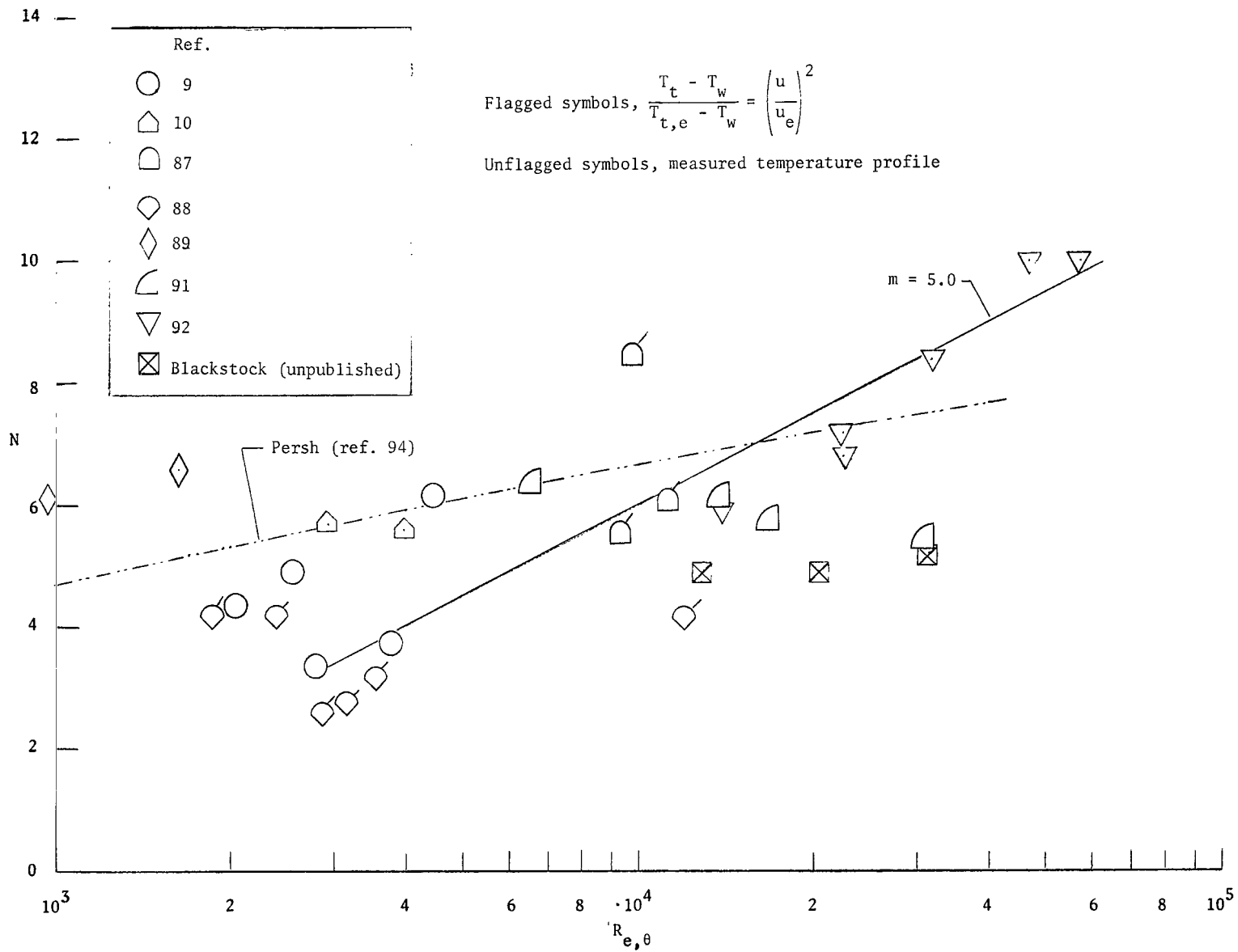


Figure 8.- Variation of N with Re, θ for axisymmetric nozzle walls at $0.12 \leq T_w/T_t \leq 0.35$. Key to symbols is presented in table III.

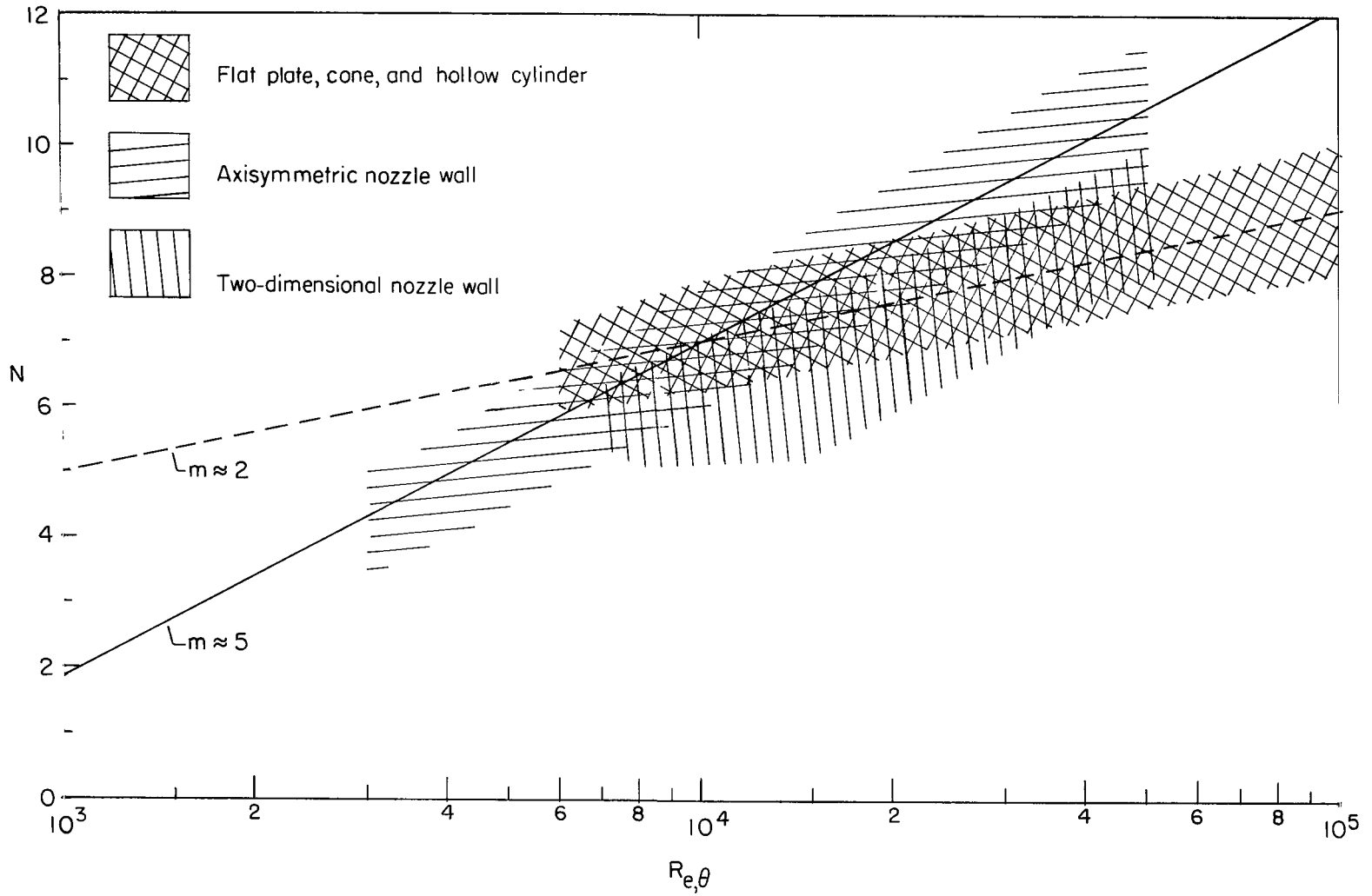
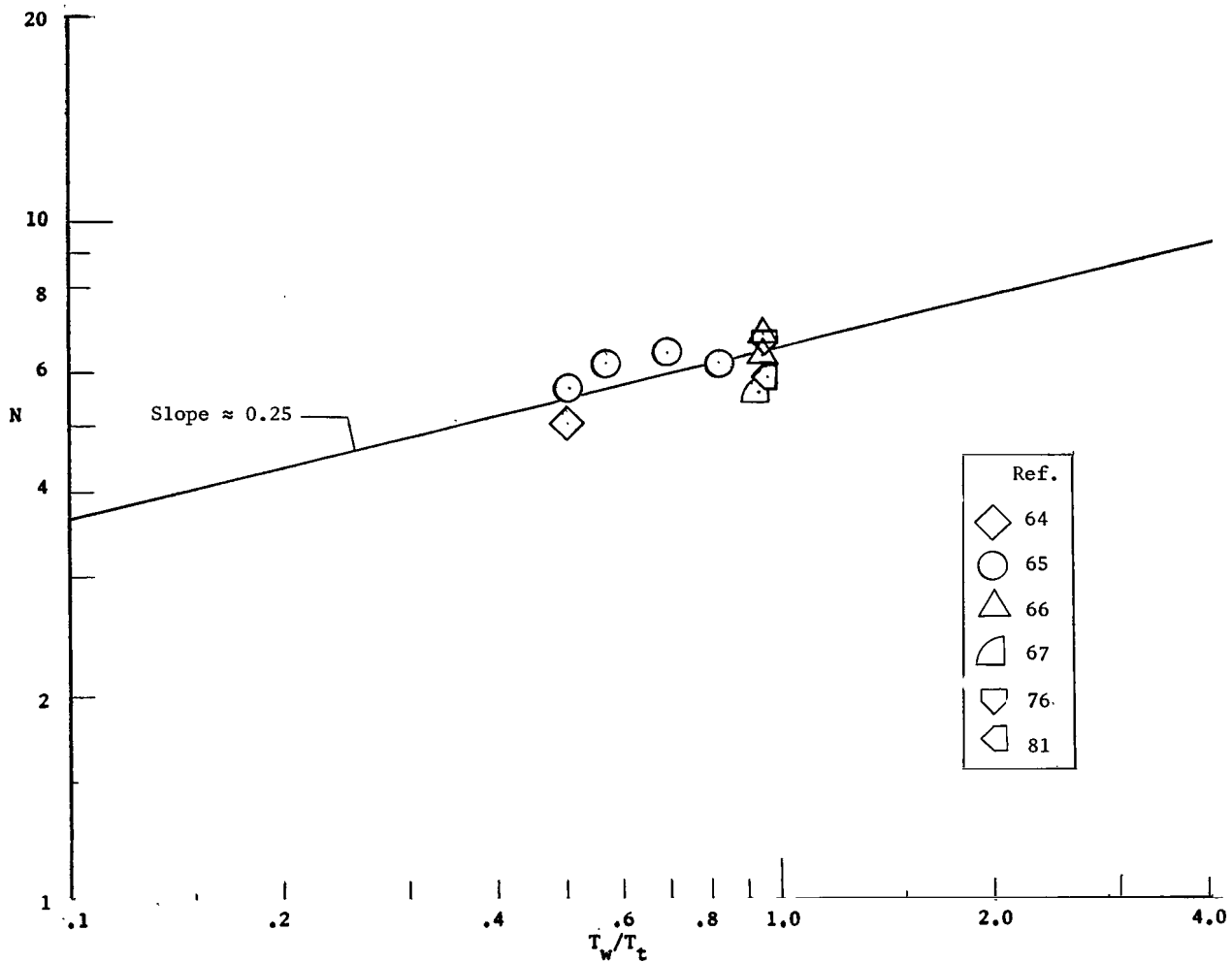
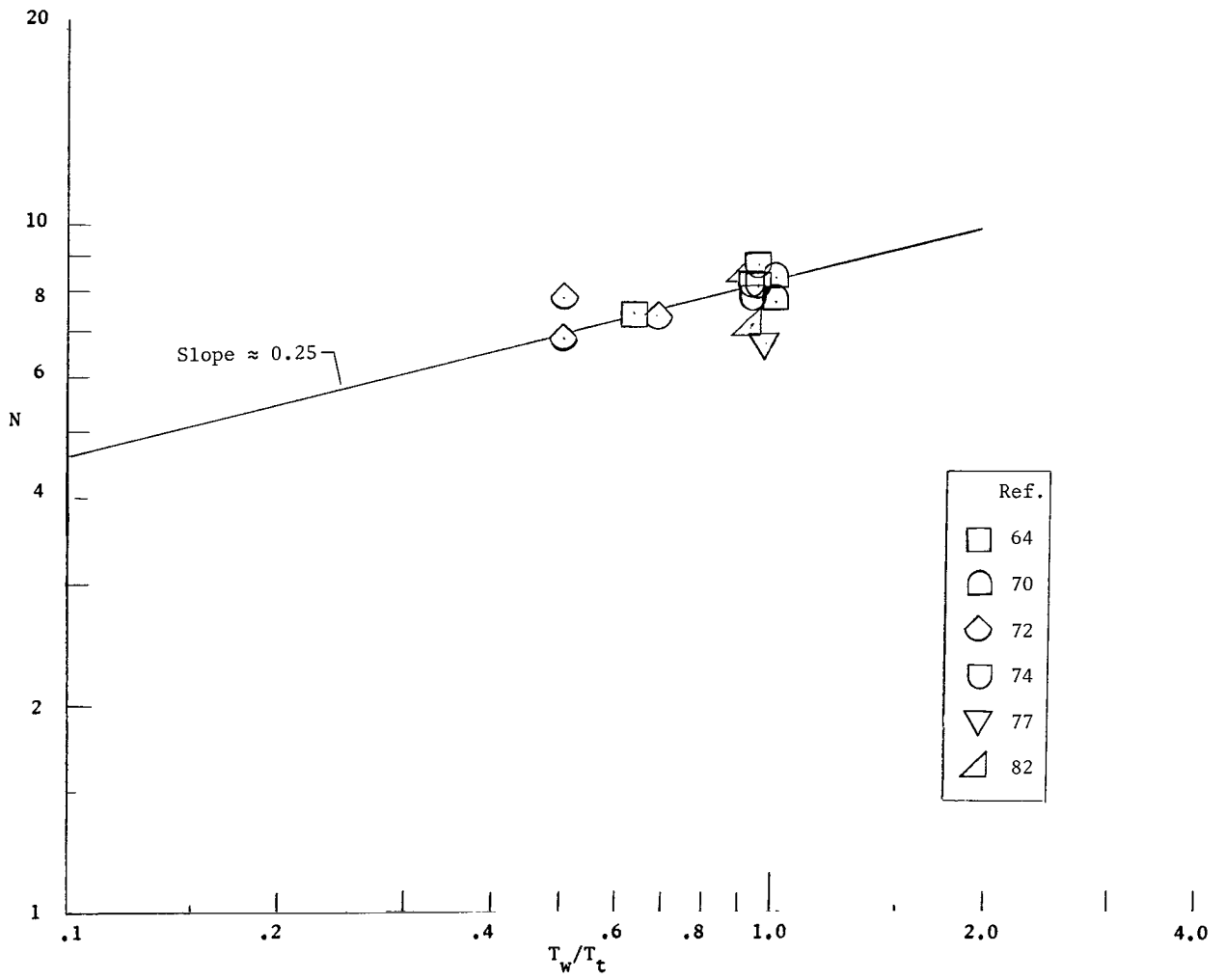


Figure 9.- Comparison of general variation of N with Re, θ for data for (1) the flat plate, cone, and hollow cylinder, (2) the axisymmetric nozzle wall, and (3) the two-dimensional nozzle wall at $0.35 < T_w/T_t \leq 0.66$.



(a) $Re_{\theta} \approx 12\ 500$; $1.81 \leq M_e \leq 10.33$.

Figure 10.- Variation of N with wall-to-total temperature ratio for two-dimensional nozzle walls at a nearly constant value of Re_{θ} . Key to symbols is presented in table II.



(b) $Re_{\theta} \approx 20\ 000$; $1.98 \leq M_e \leq 10.3$.

Figure 10.- Concluded.

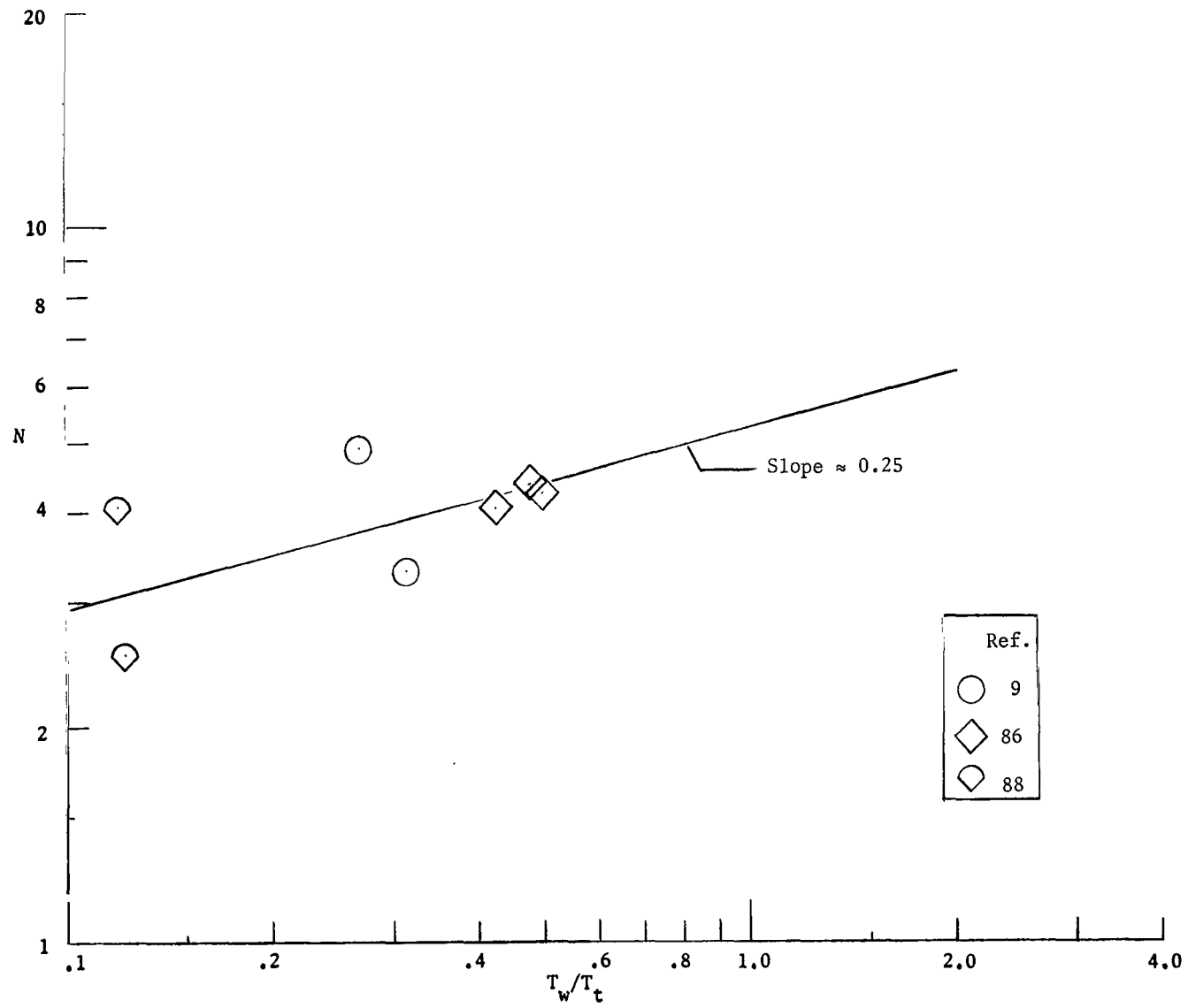


Figure 11.- Variation of N with wall-to-total temperature ratio for axisymmetric nozzle walls at a nearly constant Re_{θ} of 2500; $6.65 \leq M_e \leq 14.0$. Key to symbols is presented in table III.

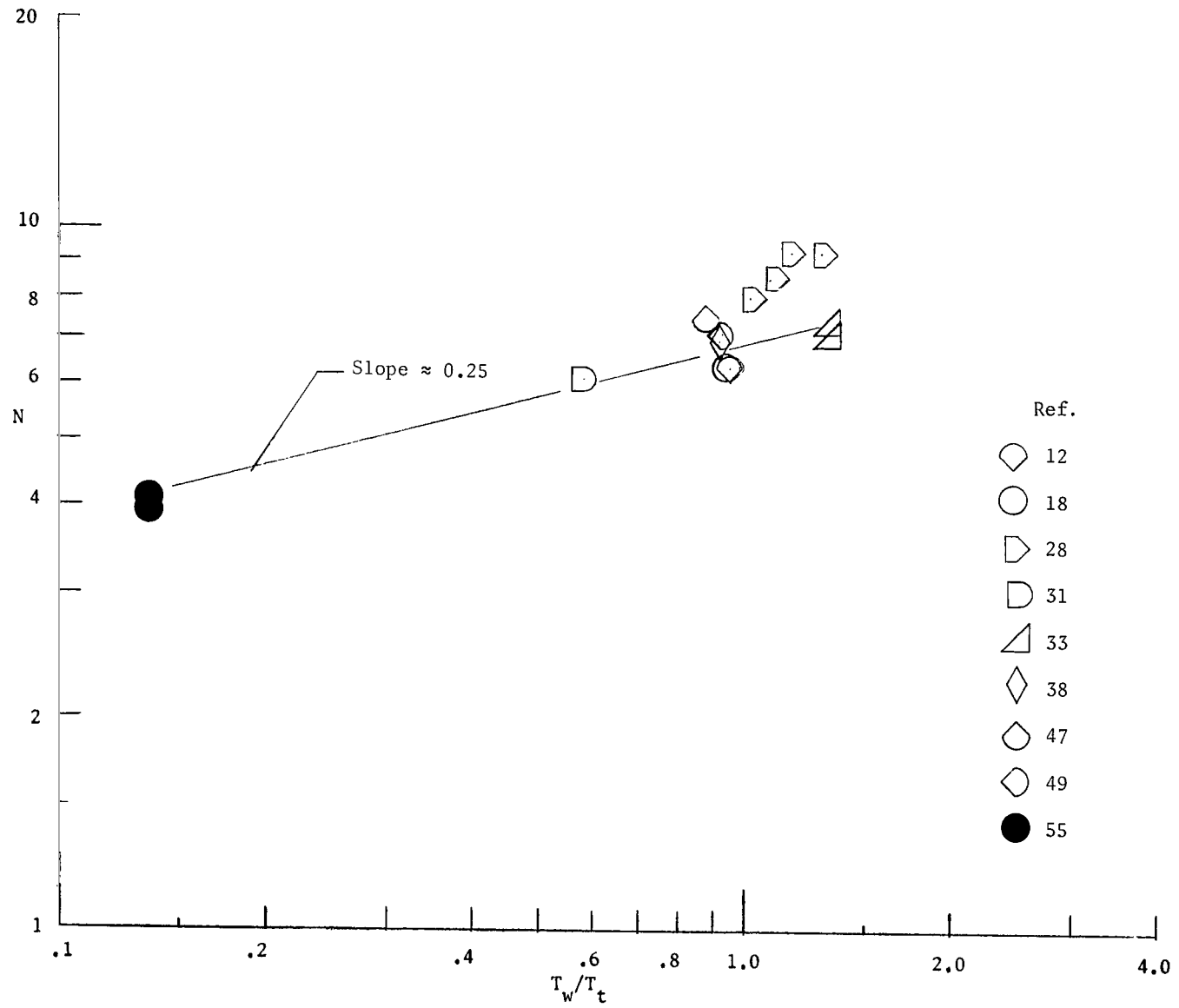


Figure 12.- Variation of N with wall-to-total temperature ratio for flat plates at a nearly constant value of Re_θ . For $T_w/T_t < 1.0$, $Re_\theta \approx 5000$; for $T_w/T_t > 1.0$, $1820 \leq Re_\theta \leq 3110$. Key to symbols is presented in table 1.

\triangle Nitrogen data; $M_e = 19.47$; $T_w/T_t = 0.17$ (ref. 10)
 \triangle Helium data; $M_e = 20.3$; $T_w/T_t = 1.0$ (Watson, unpublished)

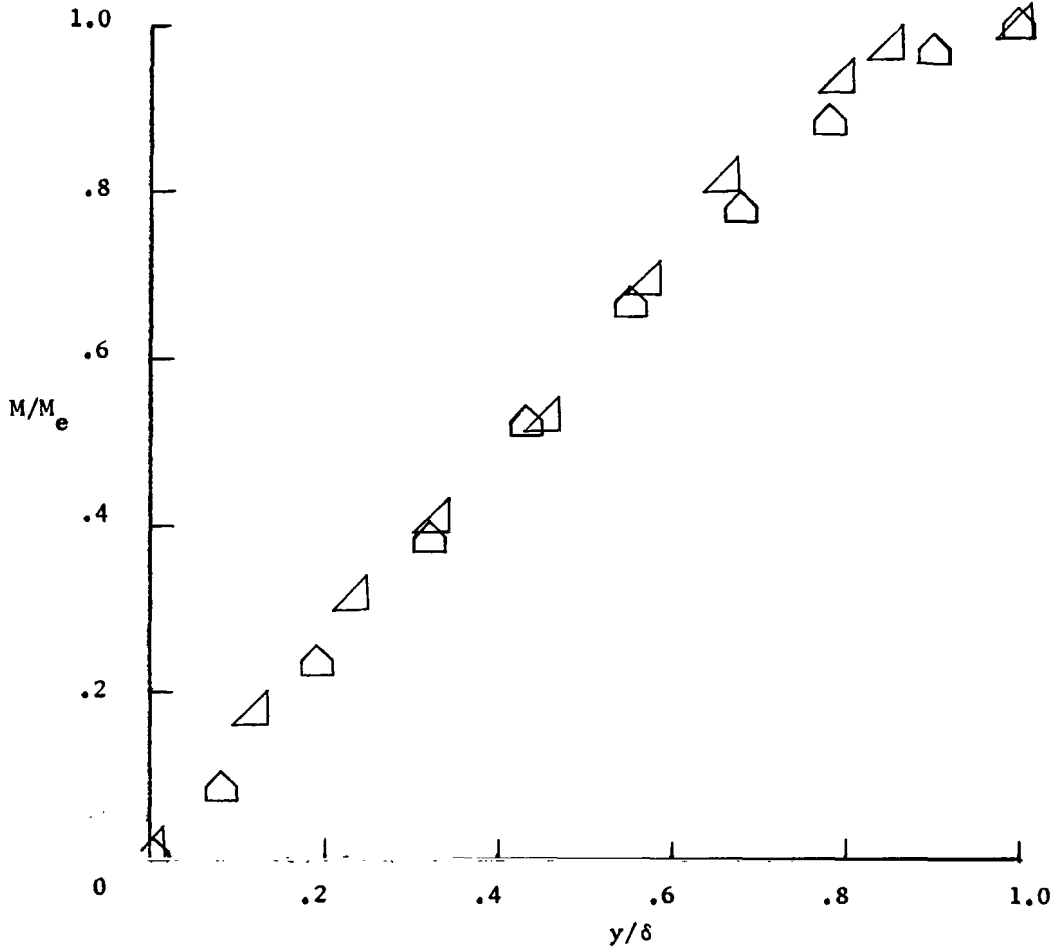


Figure 13.- Comparison of a nitrogen and a helium hypersonic turbulent-boundary-layer Mach number profile from axisymmetric nozzles. Key to symbols is presented in table III.

FIRST CLASS MAIL



POSTAGE AND FEES PAID
NATIONAL AERONAUTICS AND
SPACE ADMINISTRATION

139 001 37 5E 3DS 10075 20003
AIR FORCE WIND TUNNEL LABORATORY 761007
KEESLAND AFB, NEW MEXICO 87117

ALL E. LUD. BUD. MAN. CHIEF, FLIGHT LIBRARY

POSTMASTER: If Undeliverable (Section 158
Postal Manual) Do Not Return

"The aeronautical and space activities of the United States shall be conducted so as to contribute . . . to the expansion of human knowledge of phenomena in the atmosphere and space. The Administration shall provide for the widest practicable and appropriate dissemination of information concerning its activities and the results thereof."

— NATIONAL AERONAUTICS AND SPACE ACT OF 1958

NASA SCIENTIFIC AND TECHNICAL PUBLICATIONS

TECHNICAL REPORTS: Scientific and technical information considered important, complete, and a lasting contribution to existing knowledge.

TECHNICAL NOTES: Information less broad in scope but nevertheless of importance as a contribution to existing knowledge.

TECHNICAL MEMORANDUMS: Information receiving limited distribution because of preliminary data, security classification, or other reasons.

CONTRACTOR REPORTS: Scientific and technical information generated under a NASA contract or grant and considered an important contribution to existing knowledge.

TECHNICAL TRANSLATIONS: Information published in a foreign language considered to merit NASA distribution in English.

SPECIAL PUBLICATIONS: Information derived from or of value to NASA activities. Publications include conference proceedings, monographs, data compilations, handbooks, sourcebooks, and special bibliographies.

TECHNOLOGY UTILIZATION PUBLICATIONS: Information on technology used by NASA that may be of particular interest in commercial and other non-aerospace applications. Publications include Tech Briefs, Technology Utilization Reports and Notes, and Technology Surveys.

Details on the availability of these publications may be obtained from:

SCIENTIFIC AND TECHNICAL INFORMATION DIVISION
NATIONAL AERONAUTICS AND SPACE ADMINISTRATION
Washington, D.C. 20546